August 2016

Spectral Domain-optical Coherence Tomography for the Assessment of Cerebrovascular Plasticity

Jacob James Michael Kay
University of Wisconsin-Milwaukee

SPECTRAL DOMAIN-OPTICAL COHERENCE TOMOGRAPHY FOR THE ASSESSMENT OF CEREBROVASCULAR PLASTICITY

by

Jacob James Michael Kay

A Thesis Submitted in

Partial Fulfillment of the

Requirements for the Degree of

Master of Science

in Psychology

at

The University of Wisconsin – Milwaukee

August 2016

ABSTRACT

SPECTRAL DOMAIN-OPTICAL COHERENCE TOMOGRAPHY FOR THE ASSESSMENT OF CEREBROVASCULAR PLASTICITY

by

Jacob James Michael Kay

The University of Wisconsin-Milwaukee, 2016
Under the Supervision of Dr. Rodney A. Swain

Vascular pathologies represent the leading causes of mortality worldwide, accounting for 31% of all deaths in 2012. Cerebral hypoxia is a condition that often manifests as a result of these medical conditions. Remarkably, the nervous system has evolved mechanisms to compensate for oxygen deprivation. The dilation of existing vessels and the growth of new blood vessels are two prominent physiological responses to hypoxia, both of which play a critical role in maintaining cerebral homeostasis. More recently, exercise has been shown to induce a mild state of hypoxia in the brain, leading to several robust morphological changes within the cerebrovascular system (e.g., angiogenesis, vasodilation). Thus, exercise serves as a viable model for investigating hypoxia-induced adaptations. The present study introduces spectral domain optical coherence tomography (SD-OCT) as a novel technique for examining these micro-level changes in the rat motor cortex. SD-OCT produces high resolution, three-dimensional angiograms, and allows for moderately invasive imaging within the same animal at multiple time points. The independent effect of exercise training on cerebrovascular structure and function has never been explored using SD-OCT. Thus, the primary goal of this study was to determine the relative efficacy of SD-OCT utility. To validate this novel technology, we employed SD-OCT in the examination of exercise-dependent blood vessel growth, as well as

real-time capillary dilation in response to a laboratory-induced condition of hypoxia (i.e., 10% oxygen). In addition, histology data was collected to provide comparative measures for statistical analyses. At the start of this investigation, animals were pseudo-randomly assigned to one of two groups: 26-week voluntary exercise (VX), or an inactive control (IC). Upon completing the exercise treatment, animals were anesthetized and prepared for imaging. Vascular anatomy and blood velocity data was captured during three experimental conditions: [1] normal oxygen baseline, [2] hypoxia – 10% oxygen, and [3] normoxia, return to baseline. A two-way analysis of variance revealed a significant difference in total blood vessel density between treatment groups, independent of condition. That is, VX animals had a greater density of blood vessels in the scanned region of interest when compared to IC. These findings were confirmed using unbiased stereology techniques to analyze tissue in the scanned region of interest. Furthermore, statistical analyses revealed a significant increase in small arteriole diameter in both VX and IC animals. However, the dilation captured by SD-OCT was significantly greater in VX animals when compared to IC. In sum, exercise induces potent adaptations that promote greater flexibility during hypoxia. Moreover, these micro-level changes can be effectively probed using SD-OCT.

To

My family:

Thank you for your support and encouragement.

and to my fiancée:

Keelyn Abigail Rogers

Through the trials and tribulations of this thesis, you have been a constant source of happiness.

With love and gratitude, thank you.

"Live the full life of the mind, exhilarated by new ideas, intoxicated by the romance of the unusual." - Ernest Hemingway

TABLE OF CONTENTS

LIST OF FIGURES

ACKNOWLEDGEMENTS

First and foremost I would like to thank my mentor, Dr. Rodney A. Swain, for not only recognizing my potential to make a strong contribution to the field of behavioral neuroscience, but for providing me the tools to become a successful scientist. Thank you for guiding and supporting me over the last several years. You have set an unparalleled example for what a mentor, researcher, instructor, and academic role model should be.

I'd like to thank my collaborators at the Bio-Inspired Sciences and Technologies Laboratory, Farid Atry and Dr. Ramin Pashaie, for their contributions to this research. Both individuals are outstanding academics and without their assistance, this project would not have been possible. Thank you.

I'd also like to thank my committee members, Dr. Karyn Frick and Dr. Fred Helmstetter, for their guidance through this challenging project. Your discussion, feedback, and support have been remarkably helpful. Thank you for you invaluable advice.

Last, but certainly not least, I would like to express my gratitude to my fellow graduate students and the undergraduate research assistants who contributed to this study. You have each played an important role in shaping me as a scholar, a professional, and a human being. Thank you.

SPECTRAL DOMAIN-OPTICAL COHERENCE TOMOGRAPHY FOR THE ASSESSMENT OF CEREBROVASCULAR PLASTICITY

Vascular associated pathologies are the leading causes of fatality worldwide, killing 17.5 million people in 2012 and accounting for 3 in every 10 deaths (World Health Organization, 2014). Cerebral hypoxia is a disease state that often manifests as a result of these medical conditions, neurologic or otherwise. Underlying mechanisms are common in the neuronal degeneration resulting from acute injury (e.g., stroke, trauma, heart attack) and during progressive, adult-onset diseases (e.g., ALS, Alzheimer's disease, vascular dementia). Remarkably, the nervous system has evolved mechanisms to compensate for the lack of oxygen and glucose supply following a significant reduction or cessation of local vascular circulation (Fawcett et al., 2001; Harten et al., 2010). Blood vessel growth and vasodilation are two prominent physiological responses to hypoxia, both of which play a crucial role in neural plasticity (Zajko et al., 2009; Wang et al., 2012). Researchers suggest that these morphological changes may even protect the organism from subsequent ischemic insult (Dunn et al., 2013). Several lines of research suggest that the modulation of this neurovascular niche has vast implications in the treatment of various pathologies (Pekna et al., 2012; Riddle et al., 2003; Chen et al., 2014; Maresanu et al., 2014). Furthermore, conventional knowledge holds that exercise facilitates the blood vessel growth in the brains of both human and non-human animals (Voss et al., 2012; Thomas et al., 2012; Perrey et al., 2013). Vascular growth has largely been attributed to early stages of development (Luttun & Carmeliet, 2014). However, under certain conditions, blood vessel growth is known to occur in specific brain regions of adult animals. For example, exercise-induced angiogenesis has been shown to occur in the primary motor cortex of the adult rat (Swain et al., 2003). As a result, research pertaining to the effects of exercise on the brain has

been gaining considerable attention. Furthermore, studies suggest that exercise produces a mild state of hypoxia. Under conditions of reduced oxygen, blood vessels in the brain dilate to allow for more oxygen-rich hemoglobin to reach cell tissue (Cipolla, 2009). The compensatory mechanisms triggered by reduced vascular circulation prompt hypoxia inducible factors and the formation of new blood vessels (Berggren et al., *in preparation*).

Moreover, because hypoxic response mechanisms share similar pathways across varying degrees of reduced oxygen, exercise models should be considered another method by which to study the neurophysiological mechanisms involved in cerebrovascular associated diseases. Traditional methods of analysis (e.g., histology, immunohistochemistry, etc.) have enabled researchers to successfully examine changes in cerebrovascular architecture in response to exercise. However, these methods are not without limitations. For example, traditional histology often requires the animal subject to be sacrificed, inhibiting the collection of longitudinal data. Therefore, the amount of data that can be analyzed from each animal is limited in scope. Advanced brain imaging methods (e.g., fMRI) have allowed researchers to investigate exercise-induced changes in human brain anatomy and function at multiple time points over long periods of time. Although these methods are typically non-invasive and expand both the scope and population in which data can be collected, brain imaging is often expensive and limited in resolution. It is important to note that no single method is indisputably superior to another, as each has its advantages and disadvantages. However, spectral domain optical coherence tomography (SD-OCT) has shown promise in filling the respective gaps in both traditional analyses and established brain imaging techniques. SD-OCT produces high resolution, 3-dimensional angiograms, and allows for moderately invasive imaging within the same animal at multiple time points. This enables researchers to map the temporal sequence of

cerebrovascular adaptations in addition to real-time changes in blood vessel dilation.

Study Purpose

Taken together, the presented evidence indicates that exercise and the vasoanatomical changes that follow produce a potent neuroprotective effect. Therefore, this research project is of particular interest in the investigations of ischemia, brain injury, and neurodegeneration. Despite advancements in the field, the independent effect of exercise training on cerebrovascular structure and function has not been fully explored. Thus, using a novel imaging technique, one particular goal of this study is to examine cerebrovascular growth in the forelimb region of the primary motor cortex of the adult rat in response to voluntary exercise. An additional goal of this study is to capture real-time capillary dilation in response to a laboratory-induced condition of hypoxia-hypercapnia (i.e., 10% oxygen, 5% carbon dioxide). Using SD-OCT to examine blood vessel growth and changes in vasodilation will allow us to draw conclusions on exercise-induced cerebrovascular plasticity. Moreover, comparing the scientific application of SD-OCT with traditional methods of histology will allow us to assess its technical utility.

A Review of the Literature

The Primary Motor Cortex of the Adult Rat

The primary motor cortex is a cerebral structure that functions in the execution and control of movement. Early investigations of the primary rat motor cortex (M1) reveal a topographical organization, such that specific functional components of the body are represented within specific regions of M1. The size of the representation in M1 does not correlate with the size of the body part. Rather, the size of the representation is indicative of the number of motor neurons innervating muscle fibers in that specific region of the body. In regions that are capable

of more complex movements, such as those of the forelimb, there is a greater density of neurons within its representation in M1 (Young, Collins, & Kaas, 2013).

The topographical organization of the rodent motor cortex has been studied extensively in recent decades. Using microstimulation techniques and cytoarchitectonics, Donoghue and Wise (1982) were the first to successfully identify the relationship between the structure and functional organization of the rat motor cortex. Administration of low-intensity, intracortical microstimulation in the frontal and parietal regions of the rat brain evoked peripheral movement. The location of microelectrodes was correlated with cytoarchitecture, such that Nissl-staining revealed corticospinal projections from two distinct fields: the medial agranular field and the lateral agranular field. Stimulation of the lateral agranular field evoked significant motor movement. Fewer movements resulted from stimulation of the medial agranular field. Thus, it was determined that M1 corresponds with the lateral agranular field in the frontal region of the adult rat brain.

To this end, Neafsey and colleagues (1986) aimed to construct a detailed map of the rat motor cortex. To distinguish the subdivisions of the motor map, Neafsey and colleagues utilized similar microstimulation and histology methods as Donoghue and Wise (1982). Numerous electrodes were placed at perpendicular and parallel positions relative to the dorsal and lateral surfaces of the cortex (as shown in *Figure 1*). Electrodes in the proposed forelimb region were placed at a depth of 1.7mm. Electrodes in the proposed hind-limb region were placed at a depth of 1.5mm. These depths were chosen because this was the position where minimum threshold values were recorded (i.e., minimum stimulation to elicit movement). In thirty-two Long-Evans hooded rats, electrodes were spaced 250μm-500μm apart, allowing for a total of 300-500 electrode positions per experiment. The initial stimulation current was between 25μA and 30μA.

The current was gradually increased until a movement was produced. A 10 second pulse of 10μA of direct current was used to create marking lesions for histological reconstruction of the microelectrode tracts. Chemical staining techniques were employed to heighten the contrast of the electrode tracks relative to the background tissue, allowing the researchers to map the cytoarchitectonic coordinates of M1 subdivisions.

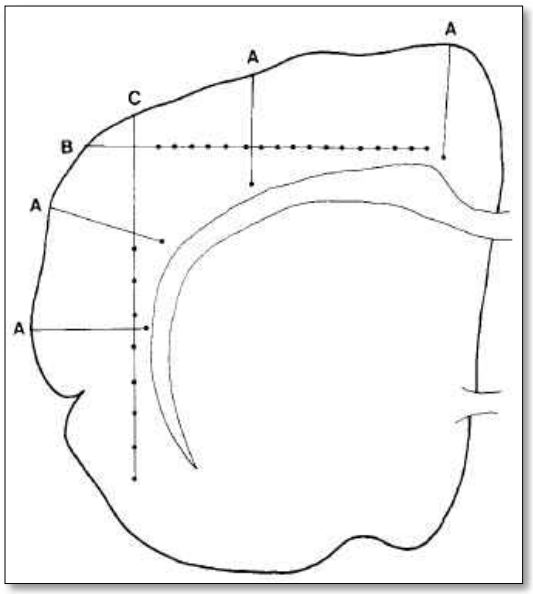

Figure 1. From Neafsey et al. (1986). Placement of microelectrodes.

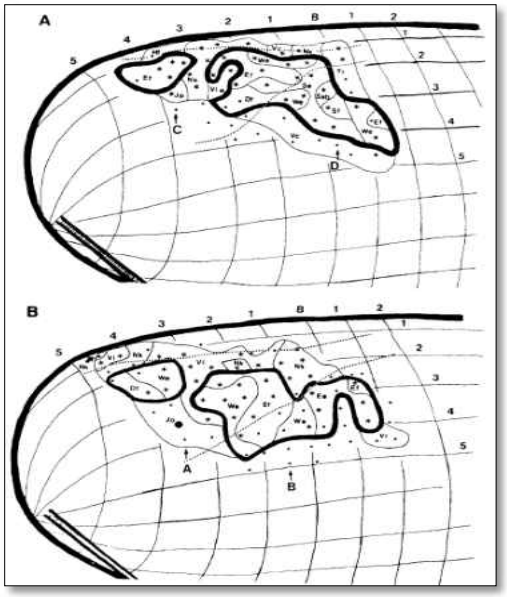

Figure 2. From Neafsey et al. (1986). Forelimb representations.

The forelimb was found to have a greater representation in M1 compared to the hind limb. As seen in *Figure 2*, an analysis of the micro-stimulation and histological data suggested that the forelimb is represented in two distinct regions: a large caudal area (~0.5mm posterior to bregma to ~3mm anterior to bregma; ~1mm to ~4.5mm lateral to midline) and a smaller rostral area located toward the frontal pole (~3-4.5mm anterior to bregma and 1-2mm lateral of midline).

In sum, Neafsey and colleagues (1990) were able to successfully map the motor cortex of the adult rat, producing a detailed schematic of the forelimb representation in M1 as well as other

regions of the body (e.g., vibrissae, jaw, tongue, lip). Electrode stimulation and histological reconstruction also indicated detailed organization within the forelimb region. For example, microstimulation of distinct areas produced movement in specific movements of the forelimb (e.g., extension and flexion of the elbow, wrist, and digits span ~1-2mm anterior to bregma).

Experiments demonstrating the topographical organization of the rat motor cortex have prompted research into its structural and functional plasticity. A variety of manipulations have been shown to result in morphological changes within motor cortex. For example, Donoghue and colleagues (1990) transected motor nerves that innervate the vibrissa. Immediately following the lesion, no movement of the vibrissae was induced upon stimulating its representation in M1. However, stimulating the same area a week post-transection evoked movement of the forelimb, providing convincing evidence of motor map reorganization. In another study conducted in 1997, G.W. Huntley observed significant changes in the functional representation of vibrissae in M1 by trimming the vibrissa of Sprague Dawley rats. Both studies indicate that peripheral manipulations of the tactile experience can significantly alter functional representations in motor cortex.

Intracortical manipulations can alter these representations as well. The pharmaceutical administration of a GABA antagonist in motor cortex decreases inhibitory circuits of adjacent representations, facilitating excitatory connections and the production of movement upon stimulation of neighboring representations (Jacobs & Donoghue, 1991). To this end, Sanes & Donoghue (2000) would later hypothesize that plasticity of the motor map reinforces the acquisition of novel motor behaviors.

Expanding upon this hypothesis, Anderson and colleagues (2002) aimed to examine morphological changes in the motor cortex of the adult rat resulting from two contextual

manipulations: acrobatic motor learning and simple repetitive exercise. The previously mapped forelimb and hind limb representations were designated as the primary regions of interest and cortical thickness of each was examined post-treatment. The rats that acquired motor skills via an obstacle course had significantly greater thickness of the hind-limb region in M1. The rats that ran voluntarily for 26-29 days had significantly greater cortical density in the forelimb representation of M1. Thus, it was concluded that regular physical exercise requires greater use of the forelimbs and increases cortical thickness in its representation in primary motor cortex. In contrast, acrobatic training requires greater use of the hind limbs and increases cortical thickness within its representation in M1.

Together, these findings corroborate evidence for experience-induced plasticity in the primary motor cortex (Markham & Greenough, 2004). However, the underlying mechanism by which the forelimb region of M1 increased in density remained unknown. One possible explanation for the observed change in cortical thickness is the exercise-induced expansion of vasculature. Drawing conclusions from Anderson et al. (2002), because the forelimb appears to dominate the physical demand during exercise and results in greater cortical expansion in its representation within M1, it should be expected that forelimb regions will show the most prominent exercise-induced blood vessel growth with respect to the other subdivisions of M1 (Kleim, Cooper, & VandenBerg, 2002). Thus, this study aims to assess the structural and functional changes in vascularity in the forelimb region of the rat M1 following chronic voluntary exercise.

Exercise-induced Hypoxia and the Brain

Recently, exercise has been shown to produce a transient state of mild hypoxia in the brain (Berggren et al., *in preparation*). Cerebral hypoxia is a condition in which the oxygen

available to the brain tissue is markedly reduced (Dugdale, 2012). Blood vessel growth and vasodilation are two prominent physiological adaptations in response to cerebral hypoxia (Michiels, 2004). Decreased tissue oxygenation prompts a cascade of molecular and cellular mechanisms to compensate for the lack of adequate oxygen supply. A host of growth factors (e.g., placental growth factor, fibroblast growth factor, vascular endothelial growth factor, etc.) are upregulated to facilitate the sprouting of new blood vessels from the preexisting vasculature (Cines et al., 1998; Pepper, 1997; Ucuzian et al., 2010). During conditions of hypoxia, enzymatic mechanisms are triggered and dilation of the blood vessel occurs (Cipolla, 2009; Patt et. al., 1997).

Angiogenesis

Early investigations of exercise-induced angiogenesis utilized histological methods to analyze structural changes in cerebellar capillaries. Black and colleagues (1990) examined the effect of physical exercise on blood vessel density in the rat paramedian lobules (i.e., forelimb region of cerebellar cortex). Results from their study indicated that rats forced to exercise on a treadmill and rats given free access to a running wheel exhibited significantly greater blood vessel density when compared to sedentary controls. In another study, Kleim and colleagues (2002) provided rats with thirty days of free access to a running wheel. An analysis of the microstimulation mapping and histology data revealed that exercised rats displayed a significant increase in vascular density within layer V of the forelimb representation in M1. The beginning depth of M1 layer V has been estimated between ±69.3μm and ±90μm with 95% confidence (Yazdan-Shahmorad et al., 2011). Providing further evidence of exercise-induced angiogenesis, Swain and colleagues (2003) found that inducing hypercapnia, a condition of elevated carbon dioxide that challenges the oxygen concentration, causes an increase in capillary perfusion of the

motor cortex. T-two-star (T2*)-weighted and flow-alternating inversion recovery (FAIR) functional magnetic resonance imaging were used to assess the changes in blood volume and flow following chronic exercise treatment. The observed increase in blood flow was significantly greater in exercised animals when compared to sedentary controls. The increase in blood volume and significant hemodynamic alterations thirty days post-exercise suggested an exercise-induced expansion of blood vessels in motor cortex. To corroborate this finding, Swain and colleagues (2003) examined the expression of the β_3 subunit (also known as CD61) of the $\alpha_V\beta_3$ integrin, an adhesion molecule that aids the sprouting of new vessels (Terry et al., 2014). The analysis of immunohistochemical data indicated that the expression of CD61 was significantly greater in exercised animals, indicative of exercise-induced angiogenesis.

Taken together, these studies provide convincing evidence for the robust vascular changes induced by exercise. These findings have prompted investigations into the underlying mechanisms of exercise-induced plasticity. Extensive research has examined the role of endothelial growth factors and cellular pathways in the production of new blood vessels, and the role of enzymatic regulation of blood vessel dilation.

Research has identified several molecular signals that are expressed in the brain in response to exercise-induced hypoxia. For example, the expression of basic fibroblast growth factor (bFGF, FGF-2), a proangiogenic factor that plays an important mitogenic role in mediating the growth of new blood vessels, has been shown to increase in the hippocampus of the adult rat following thirty days of voluntary wheel running (Gomez-Pinilla, Dao, & So, 1997). Other potent angiogenic factors, the angiopoietins (Ang1 & Ang2), play an important role in the remodeling (Ang2) and stabilization (Ang1) of the vascular system (Gale & Yancopoulos, 1999).

Moreover, the expression of both Ang1 and Ang2 has been shown to increase shortly after the commencement of an exercise regimen (Ding et al., 2004).

Two of the most extensively studied molecules are vascular endothelial growth factor (VEGF) and its transcription factor, hypoxia-inducible factor 1 alpha (HIF-1α). Both of these molecules have been shown to be upregulated in response to physical exercise (Hoier & Hellsten, 2014; Ameln et al., 2005). Angiogenesis is primarily regulated by VEGF (Ogunshola et al., 2000), and the exercise-induced expression of this growth factor is largely dependent upon hypoxia-inducible transcription factors.

Vascular endothelial growth factor acts primarily through the tyrosine kinase pathway. Fetal liver kinase 1 (Flk-1) and Fms-related tyrosine kinase 1 (Flt-1) are VEGF receptors located at the membrane of endothelial cells. When bound by VEGF the interaction signals angiogenesis (Shibuya, 2013). Although VEGF binds both of these receptors, there is evidence that their functions are not entirely similar. The Flk-1 receptor plays a predominant role in vasculogenesis, or the embryonic formation of blood vessels, whereas the Flt-1 receptor plays a crucial role in the organization and structure of the vasculature system. Shalaby and colleagues (1995) produced Flk-1 deficient mice by suppressing the Flk-1 gene, thereby inhibiting expression of the receptor. These mice failed to develop a vascular system and died during gestation. In contrast, another fundamental study provides evidence that Flt-1 is responsible for early vascular organization. By inhibiting the expression of the Flt-1 receptor, Fong and colleagues (1995) produced mice that displayed abnormal vascular structure. Similar to the mice of the Flk-1 study, these animals expired during gestation. Although the expression of these receptors is observable in the adult mammalian brain, it appears that the abundance of the Flk-1 receptor is significantly reduced into adulthood (Millauer et al., 1993), whereas the expression of Flt-1

appears to remain abundantly expressed (Peters et al., 1993). This further supports the claim that Flk-1 receptors primarily function during embryonic development and Flt-1 functions throughout the lifespan to maintain the integrity of the vascular system. Provided the evidence that VEGF is upregulated in response to exercise, it's not entirely surprising that researchers have found that the expression of both receptors is significantly increased in response to exercise (Pryor et al., 2010).

VEGF is upregulated by a host of promoters. However, the transcription factor hypoxia-inducible factor-1 alpha (HIF-1α) is one particular protein that may be unique to exercise-induced angiogenesis. Its function is dependent upon the level of oxygen available to the tissue (please reference *Figure 3* for illustration). While its purpose under normoxic conditions is not entirely understood, it has been suggested that it plays a crucial role in the maintenance of oxygen homeostasis (Stroka et al., 2001). Under conditions of normoxia, HIF-1α is rapidly

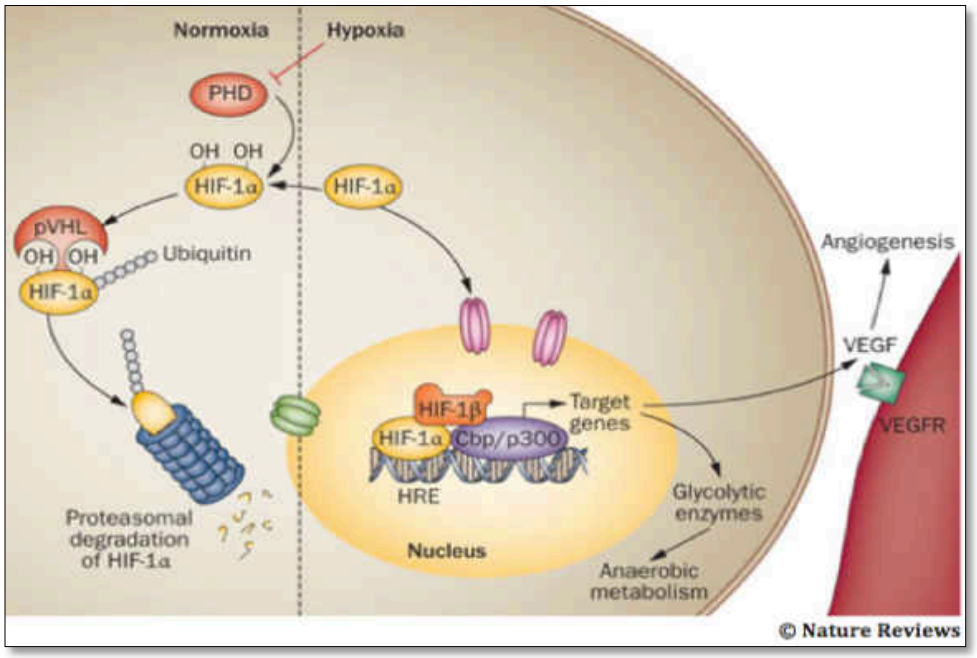

Figure 3. From Maes, Carmeliet, & Schipani. (2012). HIF-1α transcription under conditions of normoxia / hypoxia.

degraded. Prolyl-4-hydroxylase domain (PHD), a molecule that is sensitive to changes in cellular oxygenation, hydroxylates the HIF-1α complex (Salceda & Caro, 1997). This process is mediated by the von Hippel-Lindau (pVHL) tumor suppressor, which binds a chain of ubiquitin molecules to the HIF-1α complex (Nytko et al., 2007). The binding of ubiquitin signals for the HIF-1α protein's degradation (Zheng et al., 2006) via proteasomes. During conditions of hypoxia, PHD senses the reduction of available oxygen and HIF-1α degradation is inhibited. HIF-1α binds hypoxia response elements of the VEGF gene and induces the expression of VEGF molecules (Kimura et al., 2000), thereby, stimulating angiogenesis.

When VEGF binds its receptors on the endothelial cells of preexisting vessels, the cells become activated. Signals are sent to the nucleus of the endothelial cell and degradative enzymes are produced; these enzymes then create small openings in the membrane of the blood vessel (Hoeben et al., 2004). The endothelial cells then begin to divide and migrate out through the openings (Staton et al., 2009). As previously discussed, adhesive molecules (e.g., $\alpha_V\beta_3$) function like hooks to pull the sprouting endothelial cells outward from their origin. These cells then begin to fold to form a tube in which blood will later occupy (Stratman et al., 2011). Finally, supporting cells (e.g., smooth muscle cells, pericytes) form around the newly formed tubes to provide structural support and to facilitate the hemodynamic response (e.g., blood flow, vasodilation, etc.) to changes in brain oxygen demand (Ribatti & Crivellato, 2012).

Vasodilation

The dilation of blood vessels occurs when oxygen demand increases. Vasodilation allows more glucose rich hemoglobin to reach cell tissue and is regulated by numerous molecular signals (see *Figure 4*), including hypoxia-induced nitric oxide signaling (Karar & Maity, 2011). Hypoxia-inducible factors accumulate rapidly when oxygen concentration decreases, peaking

bimodally at 0 and 4 hours post-exercise (Berggren et al., *in preparation*). As previously discussed, HIFs bind to hypoxia response elements of the VEGF gene and induce the expression of VEGF molecules. One mechanism following the binding of VEGF to its receptors is the

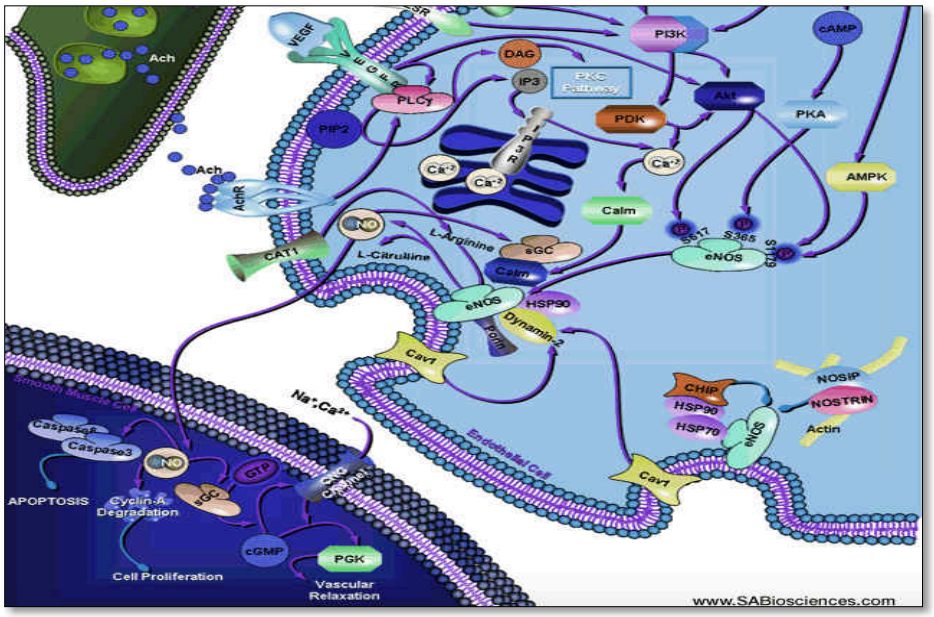

Figure 4. From SABiosciences © QIAGEN. (2015). Molecular pathways of blood vessel dilation.

stimulation of the intracellular PI3K/Akt signaling pathway, which induces the expression of endothelial nitric oxide synthase (Karar & Maity, 2011). Another, more complex mechanism involves the phospholipase-C signaling pathway (PLC- γ). When VEGF receptors are bound, PLC- γ increases intracellular calcium (Ca^{2+}), activating calmodulin (CaM), which then binds to the eNOS molecule (Dudzinski & Michel, 2007). The end result of both mechanisms is the eNOS synthesis of L-arginine to nitric oxide (NO) and L-citrulline – a molecule that can be further synthesized into additional L-arginine via argininosuccinate synthase and argininosuccinate lyase. NO then diffuses from the endothelial cell into the smooth muscle cell.

When NO accumulates in the smooth muscle cells, soluble guanylylcyclase (sGC) synthesizes cyclic guanosine monophosphate (cGMP) from guanosine triphosphate (GTP). The increasing concentration of intracellular cGMP reduces the intracellular concentration of free CA2+ by activating protein kinase-G (PKG). PKG then stimulates the production of myosin light-chain phosphatase. Dephosphorylation of myosin light-chains interferes with the cross bridge between actin and myosin, thereby, resulting in the relaxation of the smooth muscle cell (Lucas et al., 2000).

Extensive evidence shows that angiogenesis and vasodilation are two prominent adaptations to reduced oxygen concentration. It is important to examine the compensatory mechanisms by which the brain protects itself to aid advancements in the diagnosis and treatment of vascular associated diseases, and because exercise and pathologically induced hypoxia share similar molecular and cellular pathways, the behavioral manipulation of exercise presents an effective method for studying these mechanisms. Studies investigating these morphological and functional changes raise several important questions about why these adaptations occur.

Neuroprotection and Improved Cognitive Performance

One plausible explanation for the observed plasticity within the cerebrovascular system is to protect the brain tissue from ischemic injury. Blood vessels play a crucial role in supporting the neurons and other cells of the central nervous system. When the adequate supply of nutrient rich blood is disrupted, cells begin to die. Kerr and Swain (2011) showed that neurons in the hippocampus, a brain structure critical for learning and memory, began to undergo apoptotic cell death shortly after the commencement of an exercise regimen. Western blot procedures were employed to analyze the expression of caspase-3, a protein marker indicative of apoptotic cell death, in the hippocampus and cerebellum of the adult rat. From the data, the researchers were

able to determine that caspase-3 peaked roughly 24 hours post-exercise. Using similar procedures to target CD61, the researchers provided evidence suggesting exercise-induced angiogenesis peaks roughly 48 to 96 hours following running wheel exposure. Additional evidence from their study suggested that exercise facilitates the growth of new neurons in the hippocampus. Targeting DCX, a microtubule protein associated with only developing neurons, enabled the researchers to determine peak neurogenesis occurs 12 to 96 hours post-exercise. Thus, it was concluded that apoptosis is an immediate consequence of exercise; however, the system immediately responds by stimulating vessel growth, which facilitates hippocampal neurogenesis. Despite the convincing data, it remains unclear which neurons in the hippocampus expire. Perhaps exercise triggers the natural process of apoptotic cell death so that terminal stage cells within the established network are removed in order to optimize function. Or, similar to the pruning process in early stages of neurodevelopment, the newly differentiated neurons fail to make the appropriate synaptic connections and terminate. Although both are consistent with the theory of programmed cell death (i.e., apoptosis), the former seems most plausible. Nonetheless, the evidence from Kerr & Swain (2011) suggests that exercise-induced cerebrovascular plasticity has a potent influence over the proliferation of neurons.

Furthermore, the chronic exposure to mild conditions of hypoxia may strengthen the cerebrovascular system such that it becomes more resistant to ischemic insult. Dunn and colleagues (2013) conditioned rats in a chamber with a 50% reduction in atmospheric pressure (i.e., 330mmHg). This oxygen availability is similar to what would be experienced at approximately 18,000 feet above sea level, the elevation of Mount McKinley from base-to-peak. Rats were housed in the hypoxic pre-acclimation chambers for three weeks, then allowed 24 hours at near-standard atmospheric pressure to regain normal respiration and cerebral blood

flow. Lab-induced ischemia was conducted via surgical occlusion of the middle cerebral artery in the right cerebral hemisphere (MCA). The MCA supplies blood to the motor cortex as well as other frontal, temporal, and parietal regions of the brain. The bilateral asymmetry test (BAT) was utilized to assess forelimb disability. A piece of tape is placed on one forelimb of the animal, and the time it takes the rat to remove the tape with the other forelimb is recorded. The task was repeated for each limb and was conducted prior to the surgical induction of ischemia, and at 24 and 48 hours post-surgery. The duration of MCA occlusion lasted one hour before the clip and ligature were released. Magnetic resonance imaging (MRI) allowed researchers to examine the volume of affected tissue. Animals were then sacrificed and prepared for immunostaining that targeted markers for angiogenesis and inflammatory damage. Data analyses indicated that hypoxic pre-acclimation resulted in significant blood vessel growth. Additional analyses of the immunostaining data indicated a 27-45% reduction in inflammatory markers in hypoxic pre-conditioned animals. Moreover, an analysis of the MRI data provided evidence for a significant reduction in infarct volume (55%) in acclimated animals. Finally, analysis of the BAT data indicated significant behavioral improvement in acclimated animals 48 hours post-ischemia. Additionally, researchers suggest that the growth of new blood vessels facilitates the reconstruction of the damaged area. Blood vessels aid the migration of neural progenitor cells to the damaged region, and in addition, evidence suggests that endothelial cells secrete growth factors (e.g., chemokines) that aid in NPC survival (Font et al., 2010). Together, these findings suggest that the expansion of the cerebrovascular system primarily functions in the maintenance of oxygen homeostasis and the survival of neurons, and by doing so, may serve to protect the brain from future ischemic insult.

Similarly, the neuroprotective effect of blood vessel dilation has been a focus of investigation for many researchers in recent decades. Vasodilation primarily functions to maintain glucose homeostasis during conditions of reduced oxygen in the brain (Hamer et al., 1978). During conditions of reduced oxygen, NO may increase by 20x its baseline level for up to 30 minutes (Malinski et al., 1993; Sugimura et al., 1998). The presence of NO has been shown to have numerous protective benefits. Studies have shown that NO synthesized via eNOS plays a key role in vascular remodeling and the growth of new blood vessels (Papapetropoulos et al., 1997; Rudic et al., 1998; Murohara et al., 1998). For example, it has been shown that eNOS-deficient mice have significantly impaired neovascularization post-ischemia (Cui et al., 2009). Additionally, NO serves as an important inflammatory mediator, reducing the potential damage of pro-inflammatory cytokines by regulating anti-inflammatory action (Granger & Kubes, 1996). Thus, there is convincing evidence within the literature that vasodilation functions to compensate for the challenged oxygen and glucose availability during hypoxia, thereby, protecting the central nervous system from ischemic cell death. In addition, molecules recruited during conditions of low oxygen availability (e.g., NO) may be required for the post-hypoxic morphological changes to occur.

Neuroprotection is not the only advantage to these exercise-induced vascular modifications. Several lines of research suggest that exercise correlates with significant improvements in cognitive performance in both humans and non-human animals. Evidence suggests that this is true despite the age of the animal (Chae & Kim, 2009; Erickson et al., 2011; Hillman et al., 2006; Hogan, Mata, & Carstensen, 2013; Kim et al., 2010), and during healthy (Hillman, Erickson, & Kramer, 2009; Winter et al., 2007) and neuropathological conditions (Griesbach, Hovda, & Gomez-Pinilla, 2009; Kim et al., 2014). Although not directly measured

in many of these studies, there is additional evidence that vasodilation and angiogenesis largely contribute to the improvements in cognition.

Rhyu and colleagues (2010) showed that regular physical activity improves cognitive performance, and in the case of aged monkeys, improved cognition may be the result of the exercise-dependent increase in vascularity. Researchers trained monkeys to run on treadmills for an hour per day, five days a week, for five months. The Wisconsin General Testing Apparatus (WGTA), consisting of the spatial delayed response task and the object discrimination reversal task, was used to assess cognitive performance. The monkeys were transcardially perfused and the brains removed for immunohistochemical analysis. Human antibodies were used to target CD31, a cell adhesion molecule that is expressed on endothelial cells during blood vessel growth. Results indicated that, independent of age, exercised monkeys performed significantly better on the spatial delayed response task when compared to sedentary controls. Furthermore, mature monkeys (15-17 years of age) that were trained to exercise showed significantly greater blood vessel density in the motor cortex when compared to age-matched, sedentary controls.

In a study conducted with rats, Kerr and colleagues (2010) produced similar findings in support of angiogenic-dependent improvements in cognitive performance. Rats were injected with zidothymidine (AZT), a tolemerase inhibitor, to prevent exercise-induced neurogenesis in the hippocampus. An Flk-1 antagonist (SU5416) was used to inhibit exercise-induced angiogenesis. Animals received their respective injections each day during a week of voluntary wheel running. Following treatment, animals were trained on the Morris water maze (MWM), a spatial navigation task. Rats were sacrificed and immunohistochemical techniques were employed to determine the effective inhibition of neurogenesis and angiogenesis. Results indicated that animals treated with AZT performed significantly better during the acquisition

phase of the MWM task, suggesting that the growth of new blood vessels is more important for exercise-dependent learning acquisition rather than increased neuron density.

These studies indicate that the exercise-induced increase in cerebral vascularity is responsible for the improved cognition observed post-exercise. Thus, there is substantial evidence to support the claim that hypoxia-induced modifications to the cerebrovascular system not only protect the brain from ischemic threat, but also boost learning processes and improve cognitive performance. The continued examination of these adaptive mechanisms will enable us to expand upon the established theories and to better understand the normal and pathological processes associated with the cerebrovascular system, and how we can use this knowledge to improve cognitive function.

Examination of Cerebrovascular Plasticity

The incidence of vascular diseases has been increasing rapidly in recent decades. In addition, it is widely acknowledged that physical exercise leads to morphological changes in the cerebrovascular system. As a result of these phenomena, there have been numerous advancements in the techniques used to examine cerebrovascular function.

Several methods of histology have been used for decades to quantify blood vessel density in the brains of non-human animals (Berggren at al., 2014). Various stains, such as cresyl violet or toluidine blue, can be used to heighten the contrast of blood vessels in the cerebral tissue, allowing researchers to quantify vessel growth. Furthermore, immunohistochemical stains with antibodies can be used to target specific vascular proteins, enabling researchers to identify regions of the brain undergoing vascular expansion. Histological techniques are effective methods in which to examine angiogenesis, however, these methods are not without limitations. For example, these techniques often require the animal to be sacrificed and tissue is examined *in*

vitro, inhibiting the collection of longitudinal data. Thus, the amount of data that can be analyzed from each animal is limited in scope.

Advanced brain imaging techniques, such as magnetic resonance imaging (MRI) and computed tomography (CT), have enabled researchers to examine hemodynamics in conjunction with changes in vascular morphology (Raoult et al., 2014; Willems et al., 2012). Both of these imaging techniques are commonly used to produce angiograms in clinical settings to diagnose cerebrovascular abnormalities. In addition, these techniques have been implemented to investigate exercise-dependent changes in cerebrovascular function (Bullitt et al., 2009; Zeiher et al, 1995). Although these methods have proven successful in expanding both the scope and population in which data can be collected, the images produced by MRI and CT are extremely limited in temporal and spatial resolution.

It is important to note that no single method is indisputably superior to another, as each has its advantages and disadvantages. However, spectral domain optical coherence tomography has shown promise in filling the respective gaps presented by traditional histology and established brain imaging techniques. SD-OCT produces 3-dimensional angiograms equivalent in resolution to a low-power microscope (Fujimoto, 2003).

Spectral Domain Optical Coherence Tomography

Since its introduction in the early 1990's, optical coherence tomography (OCT) has quickly become one of the most widely respected techniques for imaging internal biological structures *in situ*. OCT is commonly described as "optical ultrasound." However, in contrast to ultrasound, OCT produces incredibly high-resolution images by projecting low-coherence light waves and recording the backscattered reflection of photons. Coherent waves of light maintain a constant phase difference and the same frequency. Generally, for application of OCT projects in

brain imaging the optimal spectrum is a bandwidth of 1200nm-1400nm (Kuo et al., 2013). In OCT imaging, axial (depth) resolution and the bandwidth of the light source are inversely related, such that, a larger bandwidth results in better axial resolution. Several researchers have experimented with the wavelength of the light source (Chen, 2005; Yaqoob et al., 2005; Lee et al., 2010; Ma, 2012). Generally, the longer the wavelength of the light source, the greater the reduction of scattering or deflection. Thus, light with a longer wavelength is able to form focal point deeper in tissue. Currently, OCT is limited to a depth of approximately 1mm - 2mm.

The Michelson interferometer (Michelson & Morley, 1887) is the pivotal component of the SD-OCT device. SD-OCT strikes a balance between speed and signal to noise ratio (SNR). Compared with the other OCT methods it has higher phase stability since it does not involve any mechanical movement in the reference arm, as opposed in time dependent-OCT (TD-OCT), or the light source in swept source-OCT (SS-OCT). Phase stability is particularly important in OCT velocimetry and angiography. Therefore, SD-OCT is ideal for the examination of real-time hemodynamics and OCT angiography.

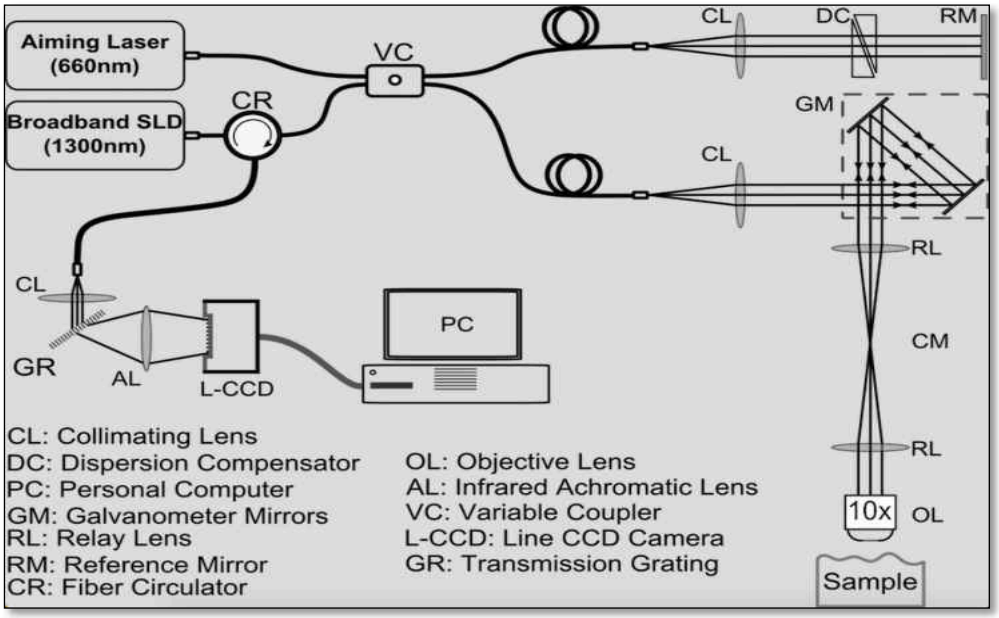

Figure 5. From Atry (2014). Schematic of SD-OCT imaging device.

The variable coupler of the interferometer (also composed of the light source, reference arm, and sample arm as seen in *Figure 5*) divides the light beam into two paths, the reference and the sample. Light waves from the reference beam project toward a reference mirror, reflect, and travel back to the relay lens. Light waves from the sample beam are projected into tissue. When these light waves come into contact with moving particles within tissue, such as red blood cells, they are scattered in all directions (Zohdi & Kuypers, 2006). Some of these photons are reflected back within the lens' field of view. The backscattered wave forms of the sample beam and the waveforms reflecting back from the reference mirror are superimposed at the variable coupler.

The recombination of these waves produces interference patterns, and this interference is captured by the detector (e.g., line charge-couple device camera). In front of this camera there is an optical grater that disperses different wavelengths of light at different angles. Each pixel within the line CCD records the interference signal of the corresponding wavelength and presents the recording as a spectrum of frequencies, ranging in intensity. Applying Fast Fourier Transform (Cooley & Tukey, 1965) to the spectral data translates the frequency intensities into a signal, namely a depth profile. Each pixel in this signal represents a depth in the sample, and its intensity is correlated to the amount of backscattered light from that depth. Simply stated, by using the interferometer, SD-OCT measures the optical length of backscattered photons in the tissue with respect to the reference surface. This is commonly known as the A-scan. By repeating this process at different transverse positions of the sample, a cross-sectional image (i.e., B-scan), or projection profile can be created. To construct the 3-dimensional image, the cross-sectional B-scans are then stacked in sequence (see *Figure 6* for illustration). By monitoring the change in the B-scans over time it is possible to capture structural and functional changes to the blood vessels in real time (see *Figure 7* for representation).

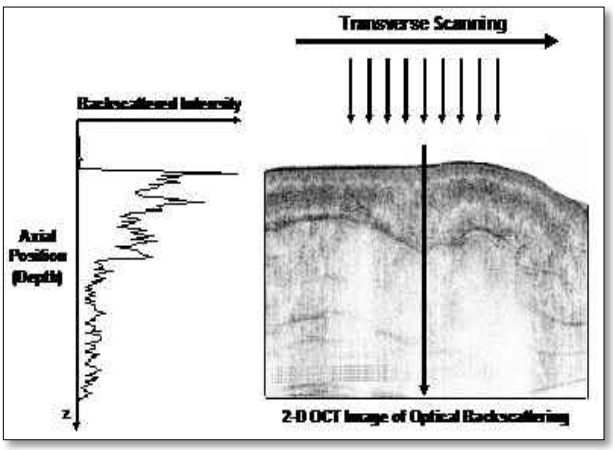

Figure 6. From Boppart et al. (2015). Diagram of transverse scan to produce the angiogram.

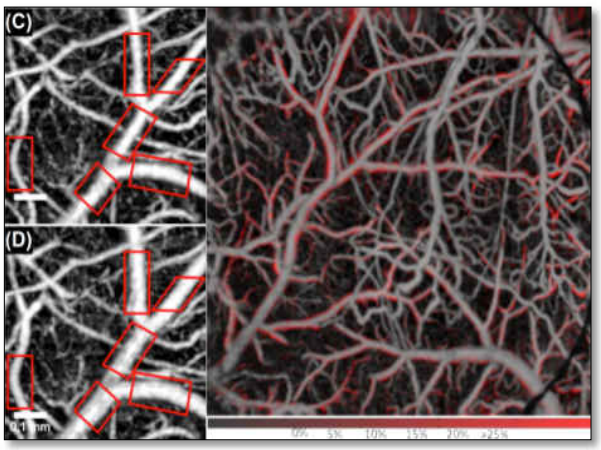

Figure 7. From Atry et al. (2014). Vasodilation during hypoxia - change in 10% O_2

An additional advantage of SD-OCT is its capacity to record changes in blood velocity. OCT velocimetry measures the shift in the wavelength of the backscattered light due to the axial velocity at each depth. This change is commonly referred to as the Doppler effect (Leitgeb et al., 2014). This has been used to measure the percent change in blood velocity (Atry et al., 2014).

Although traditional methods of analysis will continue to be incredibly valuable, the technological advancements of OCT have the potential to enhance our understanding of the underlying mechanisms of hypoxia-induced changes to the cerebrovascular system. Several features of OCT present academic and clinical advantages. For example, OCT can provide resolution approaching that of traditional histopathology in a moderately invasive manner. Its spatial and temporal resolution make it superior to the standard *in vivo* imaging technologies in use today. Albeit, Two Photon Laser Scanning Microscopy (TPLSM) provides better spatial resolution, its temporal resolution is not nearly as robust and the local injection of fluorescent dye is invasive. Furthermore, its cost-effective application makes OCT attractive in both academic and clinical settings (Libov, 2008). To date, the most significant clinical application is in ophthalmology. However, the *in situ*, real-time imaging features of OCT offer the potential

for better preoperative surgical planning and advanced intraoperative surgical guidance, thus, vastly expanding its clinical application.

Summary

Numerous studies provide evidence for exercise-induced cerebrovascular plasticity. The acute state of mild cerebral hypoxia during exercise induces a cascade of neuroprotective mechanisms. It is important to examine the compensatory mechanisms by which the brain protects itself, and because exercise and pathologically induced hypoxia share similar molecular and cellular pathways, the behavioral manipulation of exercise presents an effective method for studying these phenomena. Blood vessel growth and vasodilation are two prominent morphological adaptations following a reduction in available oxygen. These phenomena can be examined in the forelimb region of the adult rat M1 using SD-OCT. The representation of the forelimb in M1 is greater compared to the hind limb representation, and its plasticity is largely dependent upon wheel running activity. Therefore, it was determined that the forelimb region would show the most prominent increase in vascular growth with respect to the other subdivisions of M1. Research has shown an increase in vessel density in Layer V of M1 following exercise treatment. The depth of layer V (±69.3μm-±90μm) in the rat brain is well within the SD-OCT imaging window. Therefore, the forelimb region of the primary motor cortex is the optimal target for SD-OCT. The proposed study is the first of its kind. To date, SD-OCT has not been utilized to assess exercise-induced cerebrovascular plasticity.

Hypotheses

This study presents an alternative method for which to examine and understand cerebral hypoxia. A primary aim of this study was to employ SD-OCT for the assessment of long-term cerebrovascular changes in the forelimb region of the primary motor cortex of the adult rat in

response to voluntary exercise. We hypothesized that blood vessel density would be significantly greater in exercised animals when compared to sedentary controls. An additional aim of this study was to use SD-OCT to capture real-time vasodilation in response to a lab-induced condition of hypoxia-hypercapnia (i.e., 10% oxygen). We hypothesized that animals that were provided free access to a running wheel would exhibit greater vascular flexibility in response to a hypoxic-hypercapnic condition. Furthermore, an overarching goal of this study was to determine the relative efficacy of SD-OCT. Therefore, we hypothesized that certain aspects of SD-OCT will provide greater utility when compared to histological techniques.

Method

The following procedures were approved by the Institutional Animal Care and Use Committee at the University of Wisconsin—Milwaukee where this experiment took place.

Subjects

Fourteen male Long Evans—Hooded Blue Spruce rats (175-199g; approximately 3 months old) were pseudo-randomly assigned to either an inactive control (IC; $n = 7$) or voluntarily exercise group (VX; $n = 7$). Rats were ordered from Harlan Laboratories of Indianapolis, Indiana. Upon arrival, all animals were placed singly in standard shoebox cages without enrichment. Social housing and exposure to environmental stimuli (i.e., enriched environments) are known to influence brain plasticity (Markham & Greenough, 2004), and these events could potentially confuse the interpretation of the results. Therefore, to avoid confounding conditions and to be certain the observed morphological changes in the brain were the result of the experimental manipulation, animals were housed individually with no environmental stimuli. Furthermore, each rat was acclimated to handling through 5-minute daily interactions during the week prior to the onset of the exercise regimen. Animals were housed in a

temperature-controlled room, provided with food and water *ad libitum,* and were exposed to a twelve-hour light/dark schedule.

Treatment Conditions

Animals assigned to the voluntary exercise (VX) condition were provided voluntary access to a running wheel (14in. diameter) for an average of 26 weeks. During exercise treatment, animals were checked and weighed each day to ensure that they were tolerating the treatment well. No animals were removed from the study for health concerns. Wheel revolutions were recorded daily for quantification and statistical analysis. Following exercise treatment, animals were anesthetized and prepared for imaging. Animals assigned to the inactive control (IC) condition remained sedentary for an average 26 weeks. Following an average 26 weeks of no activity, each control animal was anesthetized and prepared for imaging.

In Vivo Analysis

Three-dimensional angiograms and blood velocity profiles were obtained by using a custom-made spectral domain optical coherence tomography system. This system uses a light source at the central wavelength of 1,300 nm and spectral bandwidth of >170nm to produce a depth resolution of ~5μm within a maximum 2x2x1.6mm^3 (xyz) volumetric scanning field. A 10x objective was used to provide a lateral resolution of ~4μm.

Animal preparation

In preparation for SD-OCT analysis, animals were anesthetized using 4% induction v/v isoflurane in a gas mixture of 80% air and 20% oxygen. Heart rate and blood oxygen saturation was monitored with a pulse oximeter (Pulsesense^{TM} VET 2014, Nonin Medical, Inc., Plymouth, Minnesota, United States) throughout the duration of surgical and experimental procedures. The head of each rat was then fixed in a stereotaxic apparatus. The scalp was retracted and a Dremel

tool with a dental burr was used to thin a ~3 x 3mm^2 skull region over the right forelimb representation (left hemisphere) in primary motor cortex to translucency. The thinned skull section and underlying Dura mater were then removed with a tissue forceps. The objective lens of the SD-OCT scanner was then situated and secured over the identified region of interest. One experimental animal expired during the initial administration of anesthesia. Due to excessive bleeding, two additional animals (one control, one experimental) expired during surgical procedures. In one experimental animal, it was necessary to expose motor cortex of the right hemisphere due to incessant bleeding in the left region of interest.

SD-OCT angiography & SD-OCT Doppler

Administration of isoflurane persisted throughout the duration of each scanning session. Sedation was maintained with 1.5 – 2.5% v/v isoflurane in normal air (~20% oxygen) for the baseline and normoxia conditions, and in a mixture of nitrogen (85%), oxygen (10%), and carbon dioxide (5%) gases during the hypoxia condition. The animal's core temperature was maintained at 37°C using a heating blanket. Each rat was subjected to a total of three scanning conditions, each producing 2-4 angiograms and one Doppler flowmetry image. The initial baseline set of scans occurred during normal oxygen conditions. For the second set of scans, oxygen levels were manipulated from normoxia (~21% oxygen) to a hypoxic-hypercapnic condition of 10% available oxygen and 5% carbon dioxide. For the final scanning condition, gas levels were returned to normoxia. The duration of each scanning condition (baseline, hypoxic-hypercapnic, normoxic) lasted approximately 30-45 minutes. Two experimental animals died following the last scan of the hypoxia condition. An attempt to recover the animals by returning normal oxygen was unsuccessful. Thus, collection of data during normoxia for these two animals was impractical. SD-OCT data was successfully collected during baseline and hypoxia

in 11 (5 experimental, 6 control) of the 14 animals, and through the final condition of normoxia in 9 (3 experimental, 6 control) of the 14 animals.

During scanning, the SD-OCT device did not touch the tissue; rather, it scanned a field of view with about 3mW of near-infrared light with a wavelength of approximately 1300nm. This range is an acceptable level and has been used before in published manuscripts (Atry et al., 2014). During each scanning condition, SD-OCT allowed us to capture real-time Doppler images and locate vessels and capillaries in each of the corresponding cross sections (B-scans) by adjusting the field of view of the scanner. For angiographic imaging, cross sections within a *2mm x 2mm* scanning field were imaged 10 times before moving to the next cross-sectional position (B-scans). Each B-scan consisted of 650 A-scans. This procedure was repeated for 650 cross sections resulting in 6500 B-scans over the 2mmx2mm field of view. During the scanning, data gathered from the backscattered photons produce depth profiles of the tissue in real-time. These depth profiles were displayed on a monitor adjacent to the scanning device (see *Figure 8*).

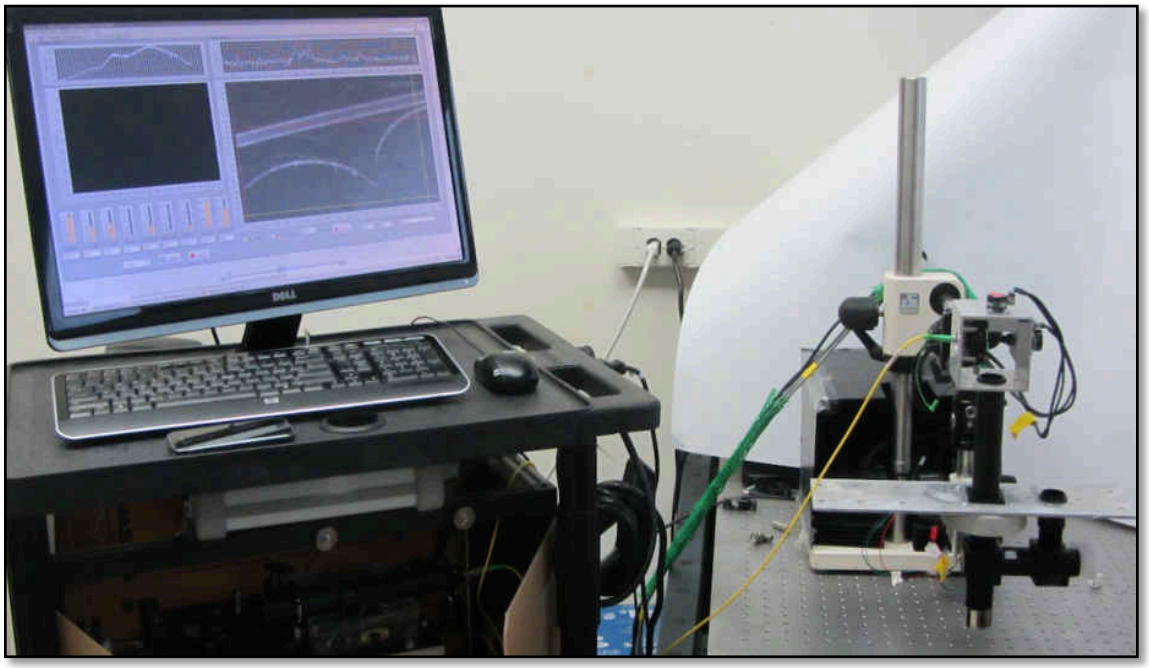

Figure 8. SD-OCT scanning device (right) and adjacent monitor (left)

This allowed us to estimate imaging depth and observe any possible obstructions (e.g., remaining meningeal layers dorsal to the subarachnoid space). For velocity (Doppler) measurements, the total of 500 cross sections were scanned at repetition of 1 B-scan per cross section. Each B-scan consisted of 3000 A-scans.

SD-OCT image processing & analysis

Using MATLAB software, Fast Fourier transform (Cooley & Tukey, 1965) was applied to the interference patterns recorded at each lateral position to obtain a depth profile of the tissue. Concatenating depth profiles of each B-scan provided a cross-sectional image. To produce a cross-sectional angiogram at each position, a local motion compensation algorithm followed by a phase-sensitive angiography technique was applied to the 10 B-scans that were recorded from each cross section. During the local motion compensation algorithm the first B-scan is being used as a reference and each of the other B-scans are divided into clusters of five A-scans. Within each cluster, the corresponding position in the reference B-scan that produced the maximum cross-correlation was found. After motion compensation, the average difference between all 10 B-scans is calculated. The total number of 650 cross sectional images were calculated over an area of *2mm x 2mm*; each cross section consisted of 650 lateral positions. After stacking all cross-sectional scans to form the volumetric angiogram, a 3D blurring kernel was applied to reduce the noise and then the two-dimensional maximum intensity projection of the angiograms was obtained. Adaptive histogram equalization (MATLAB and Image processing toolbox Release 2012b, The MathWorks, Inc., Natick, Massachusetts, United States) was applied to improve the contrast of maximum intensity projection images. This process was repeated following each subsequent scanning session. It was determined that the resulting angiograms from one control animal were not suitable for further analyses due to inadequate resolution. It is

suspected that an unidentified obstruction prevented the SD-OCT from adequately recording data. Although not apparent on the SD-OCT monitor prior to scanning, it is possible a thin layer of *dura mater* remained and blocked the recording of backscattered light.

For blood velocity measurement, the tissue was scanned at 3,000 A-scans per cross section, totaling 500 tissue cross-sections at a rate of 40,000 A-scans per second. At each cross sectional position, the Doppler shift introduced by the moving particles was estimated by calculating the average power spectrum density of the signal, which consisted of seven consecutive OCT signals at each scanned position. However, during processing of the Doppler data, it was determined that image resolution was low quality and too inconsistent to warrant statistical analysis. We speculate that the time point in which the data was collected (e.g., the last scan during each condition) was problematic. During each scanning condition, blood accumulated over the scanning region of interest. In addition, inflammation progressed and likely shifted the focal plane of the lens, compromising the collection of usable Doppler data.

Angiogram data from each animal was then coded in order to keep evaluators blind to the treatment conditions during vessel quantification. For each angiogram, density measures were collected using methods similar to image analysis conducted during unbiased stereology (Mouton, 2002). Images were formatted in ImageJ (Rasband, 1997-2016) and a point grid was superimposed on the image (see *Figure 9*, pg. 32). Vessel size categories (small, medium, large) were subjectively determined prior to evaluation. Points that fell on a vessel were counted, noted for size, and divided by total number of points within the region of interest. The area fraction provided a measure of blood vessel density, and the resulting measures for each image were averaged by condition. This allowed us to statistically analyze the mean percent area occupied by blood vessels in each of the experimental conditions within treatment and control groups.

Vessel diameter was measured in a 600-point subsample equally representing each size category to determine change in dilation across oxygen status conditions.

Traditional Histology

Tissue preparation

Following the completion of scanning procedures, each animal was anesthetized via immersion in an isoflurane chamber and monitored for respiratory arrest. Once breathing had ceased, the chest cavity was opened to expose the heart. The animal was then transcardially perfused with a ventricular catheter. A 0.1M phosphate buffer solution was administered with the force of gravity through the ventricular catheter until adequate perfusion was achieved. Following the buffer solution, 200ml of warmed (37°C) standard India ink solution was delivered through the ventricular catheter using a single-syringe infusion pump.

The brain of each rat was then extracted and post-fixed in a 4% paraformaldehyde solution for twenty-four hours. Each brain was then immersed in a 30% sucrose solution for approximately 24 hours or until adequate cryoprotection was achieved. The region of motor cortex previously scanned using SD-OCT was dissected and prepared for slicing. Using a Leica CM 3050 S cryostat (Wetzlar, Germany), each brain was sectioned at 40µm thick slices. Tissue slices were randomly selected, mounted to microscope slides, coverslipped, and prepared for vessel quantification.

Tissue analysis: Unbiased stereology

Unbiased stereology (Mouton, 2002) was utilized to quantify blood vessel density in each slice from the selected region of interest. A variation of the Dissector technique of point counting was employed (Berggren et al., 2014). Briefly, tissue slices were imaged at 400X magnification with an Olympus BX41 microscope fixed with a SPOT insight digital camera

(Version 4.5.7). Tissue samples from each animal were coded to ensure that evaluators were blind to experimental conditions. Images were captured in non-overlapping fashion to avoid sampling bias. Using a random number generator, a subset of images was selected for analysis. The coded images were then formatted in ImageJ (Rasband, 1997-2016) and a point grid was superimposed on each image (see *Figure 10*). Points that fell on a vessel were recorded. The total number of vessels in each category were counted and divided by total number of points within the region of interest. This area fraction provided a measure of categorized blood vessel density, allowing us to analyze statistical differences in the mean percent area occupied by capillaries and other sized blood vessels between the treatment and control conditions. During this analysis it became clear that only the capillaries (~3-10µm in diameter) had retained the India ink stain. We speculate that the smaller diameter of the capillaries prevented the India ink from "washing out" during Pur-Mount and coverslip application. Despite a lack of endothelium staining, larger vessels were clearly visible at 400X magnification. Thus, vessels were again categorized by size (e.g., capillary, small vessel, medium, and large).

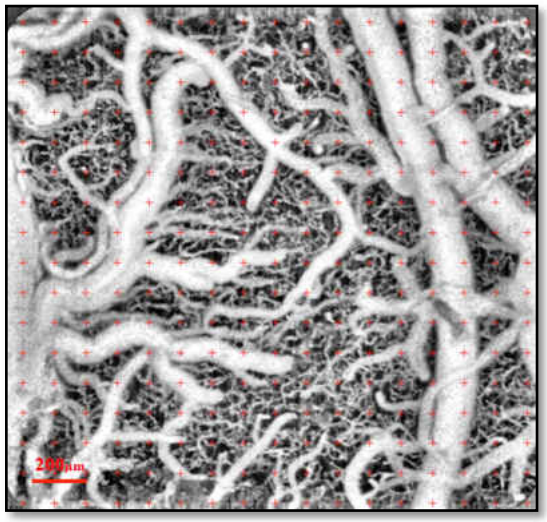

Figure 9. SD-OCT angiogram with point grid superimposed. Scale bar is 200µm.

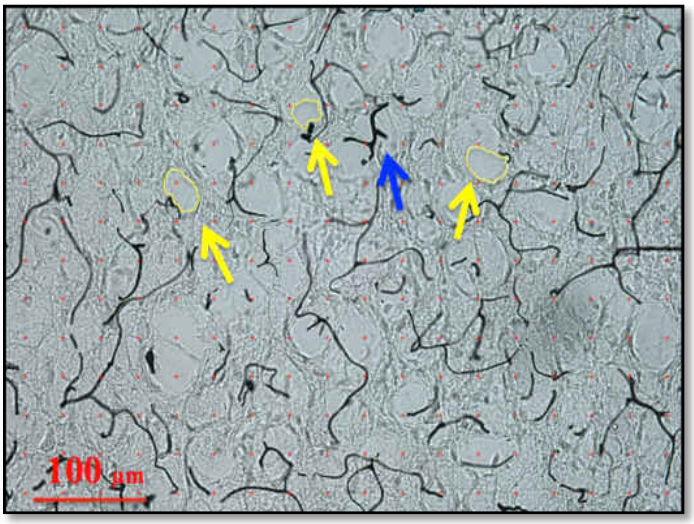

Figure 10. Histology image with capillaries (blue) and small vessels labeled (yellow). Scale bar is 100µm.

Statistical Analyses

For analyses, a repeated measures posttest design with non-equivalent control was employed. Treatment manipulation (exercise or control) and oxygen availability (hypoxia or normoxia) served as the independent variables. The change in vessel density was dependent upon the randomly assigned treatment condition. The change in vessel diameter was dependent upon oxygen availability and the assigned treatment condition. A two-way repeated measure ANOVA was conducted for each size category and all sizes combined to determine significant differences in the mean percent area occupied by vessels in the processed SD-OCT angiograms. A separate two-way repeated measure ANOVA was conducted to examine differences in the mean percent change in blood vessel dilation captured by SD-OCT. For comparison, independent- and paired-samples t-tests were conducted in order to determine significant differences in the mean percent area occupied by vessels in the collected tissue samples.

RESULTS

Two experimental animals and one control animal were lost during animal preparation procedures (VX4 – V3H1M, VX6 – G0K2A, and IC1 – G1O6M). Two additional experimental animals (VX1 – U0Z7J and VX3 – N5L5X) expired following the last scan of the hypoxia condition, leaving a total of nine animals (three experimental and six controls) that completed all phases of the study. SD-OCT angiograms from one animal (IC4 – I0F5T) were not used in the analysis due to the poor quality of the processed images. Baseline and hypoxia angiograms from ten of the fourteen animals were included in the analyses. Due to a low number of experimental animals completing all phases of the study, group means supplemented missing data for the blood vessel density ANOVA. The analysis for average change in vessel diameter from hypoxia back to baseline was not conducted. This data comprised a subset of vessels from the larger

sample and due to the low number of experimental animals to complete all three oxygen conditions, only a few VX animals produced viable data during the final normoxia phase of the study. Due to low resolution, the Doppler images were not analyzed.

Running Behavior

Animals averaged approximately 1380 revolutions each night over the first seven days they had access to the running wheel. Weekly revolutions increased rapidly ($y = 580.65x + 1543.7$, $R^2 = 0.76866$) over the first several weeks until reaching a peak average of 5343 revolutions per night during the seventh week (see *Figure 11*). The circumference of the wheel was calculated at 43.982 inches (3.665 feet). During their peak running week, animals averaged 3.71 miles per night. Weekly revolutions then decreased gradually ($y = -142.94x + 4226.4$, $R^2 = 0.74509$) until reaching near baseline levels at the conclusion of exercise treatment. On some days, the digital revolution counter became disconnected. Data from the previous day and the day after were averaged to estimate missing values.

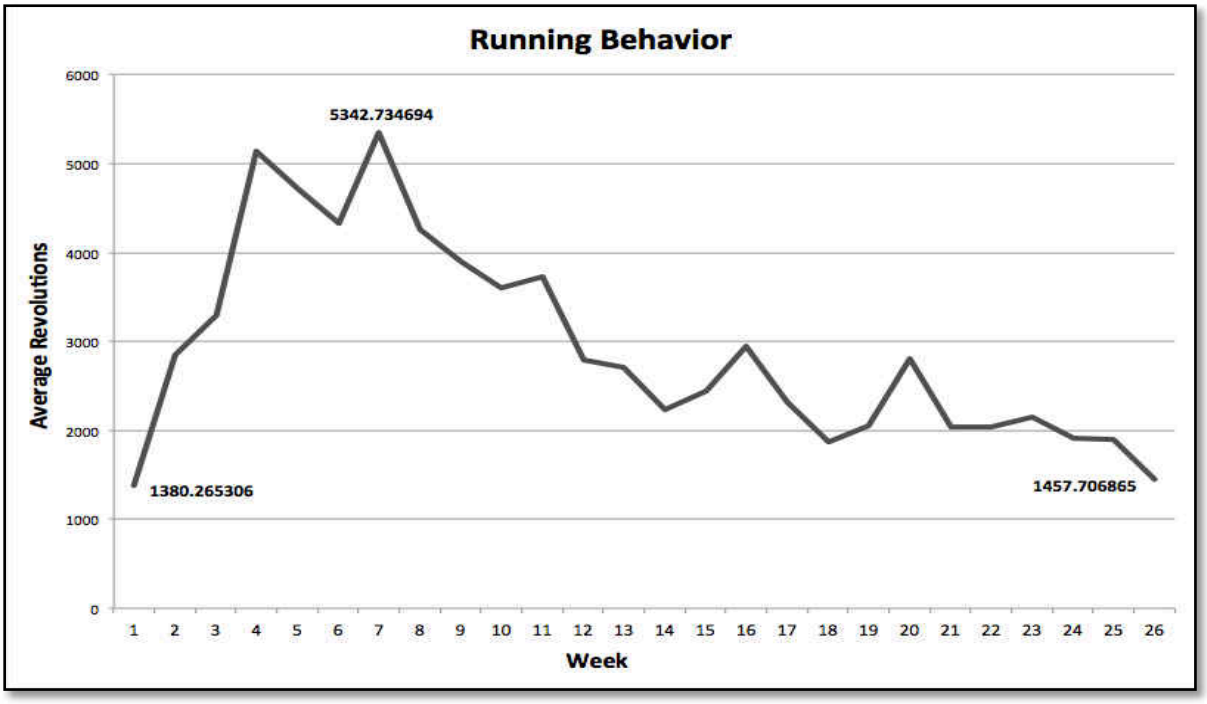

Figure 11. Running behavior over the average 26-week exercise treatment.

SD-OCT: Blood Vessel Density

Total blood vessel density (i.e., capillaries, arterioles/venules combined) was found to be greater in exercised animals when compared to inactive controls (see *Figure 12*). The two-way repeated measures ANOVA did not reveal any significant group x condition (baseline, hypoxia, normoxia) interactions when different sized vessels were analyzed independently or when size categories were combined into total blood vessel density ($F_{(2,7)} = 2.176$, $p = 0.184$). In addition, there was no main effect for condition in any size category independently or when combined into total blood vessel density ($F_{(2,7)} = 1.561$, $p = 0.275$). This suggests that blood vessel density, regardless of size, was not associated with a change in oxygen status. However, the analysis indicated a significant main effect for group ($F_{(1,8)} = 5.311$, $p = 0.050$) when all vessel size categories were combined, suggesting that total blood vessel density was dependent upon which group the animal was assigned. That is, VX animals had significantly greater blood vessel density ($M = .518$, $SD = .057$) when compared to IC ($M = .469$, $SD = .079$).

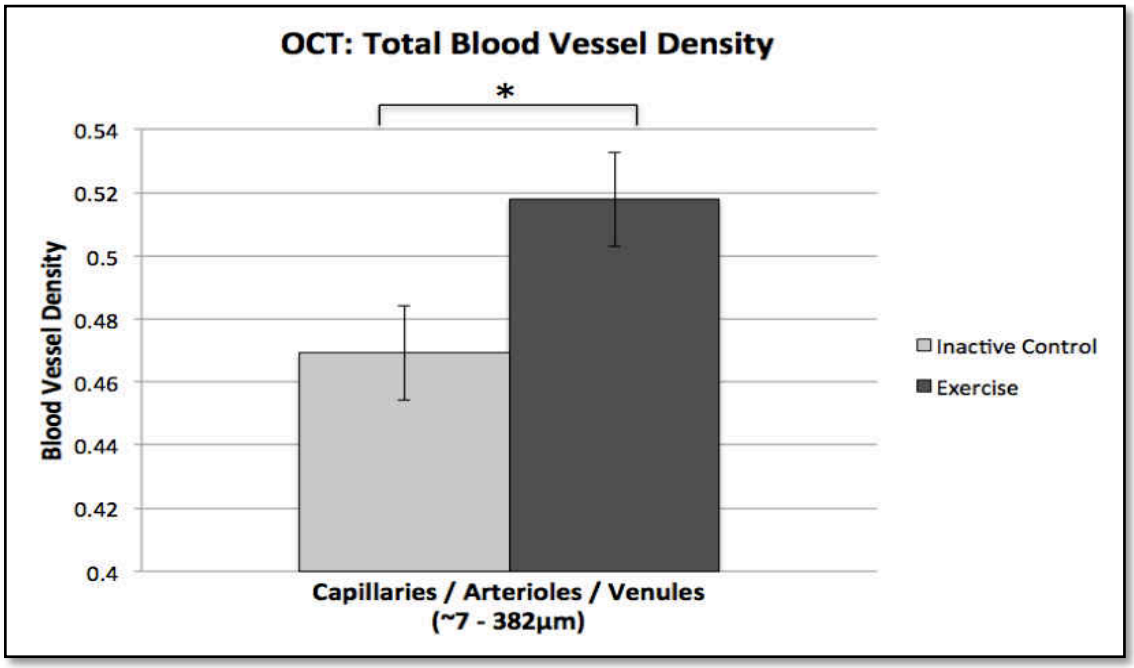

Figure 12. Blood vessel density with all size categories included. The group main effect for total blood vessel density was statistically significant (* $p = 0.05$)

SD-OCT: Vessel Dilation

A subset of vessels (n =10) of each size (small, medium, large) was sampled from each animal. Diameter was measured in baseline images and at the same position in hypoxia images; the change (Avg. $diameter_{hypoxia}$ – Avg. $diameter_{baseline}$) was recorded. The small vessels of both exercised and inactive control animals were significantly dilated during hypoxia; however, the percent change was significantly greater in VX animals. Results from a two-way repeated measures ANOVA revealed a significant group x condition interaction ($F_{(1,8)} = 7.643$, $p < 0.05$) for small vessels, suggesting that small vessel dilation is dependent upon the interplay of these two factors. A significant main effect for group ($F_{(1,8)} = 22.338$, $p < 0.001$) and a significant main effect for condition ($F_{(1,8)} = 49.599$, $p < 0.001$) were observed. As seen in *Figure 13*, the results indicate that the average percent change in small vessels diameter of VX animals (M = .1164, SD = .04) is significantly greater than the change observed in IC (M = .0657, SD = .04).

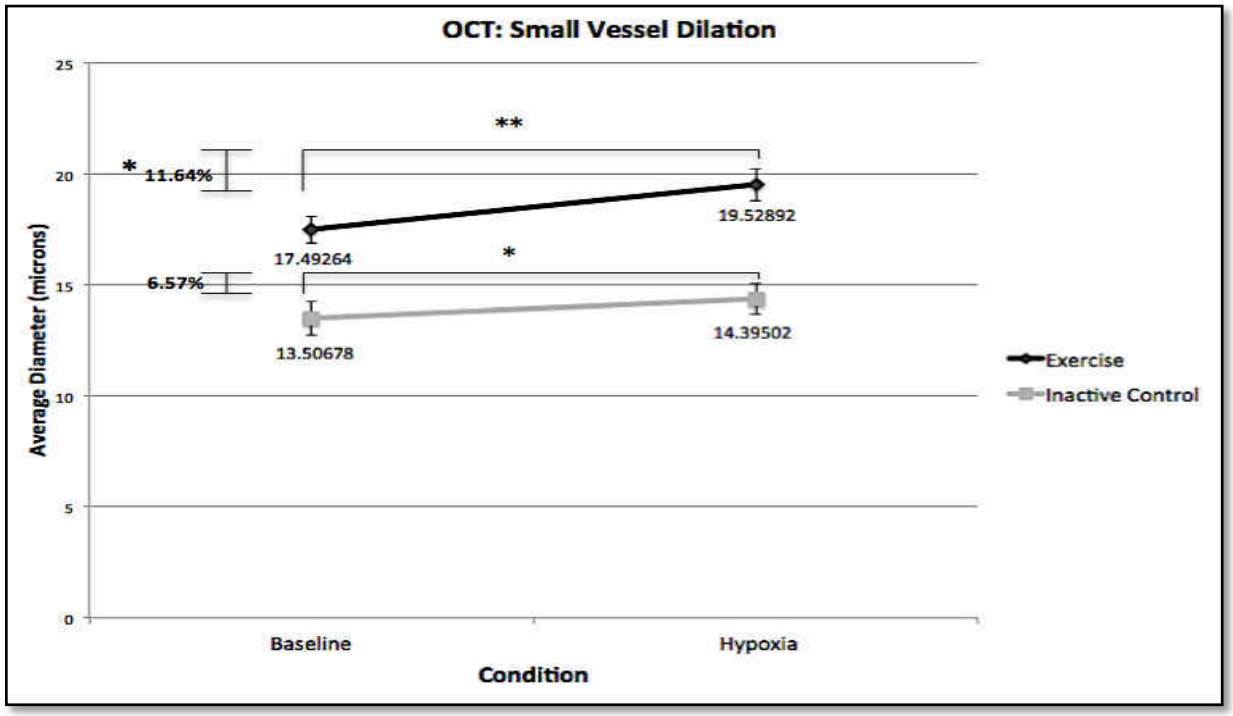

Figure 13. Small vessels for both group dilated significantly during hypoxia; however, small vessel dilation significantly greater in VX animals (* $p < 0.05$, ** $p < 0.005$)

There were no statistical differences in the average change of vessel diameter within or between groups for the other size vessels (i.e., medium or large vessels). In addition, the normoxia condition was excluded from this analysis. Given that this data was obtained from a much larger sample, supplementing means for the low number of experimental animals that completed the final normoxia phase of the study was unfitting.

Histology: Blood Vessel Density

The histology data was collected using a variation of the Dissector technique from methods of unbiased stereology (Mouton, 2002). Analyses revealed significantly greater blood vessel densities in VX animals when compared to IC. Results from an independent-samples t-test indicate a significantly greater ($t_{(12)} = 3.936$, $p = .002$; *Figure 14*) total blood vessel density in VX ($M = .319$, $SD = .087$) when compared to IC ($M = .186$, $SD = .018$).

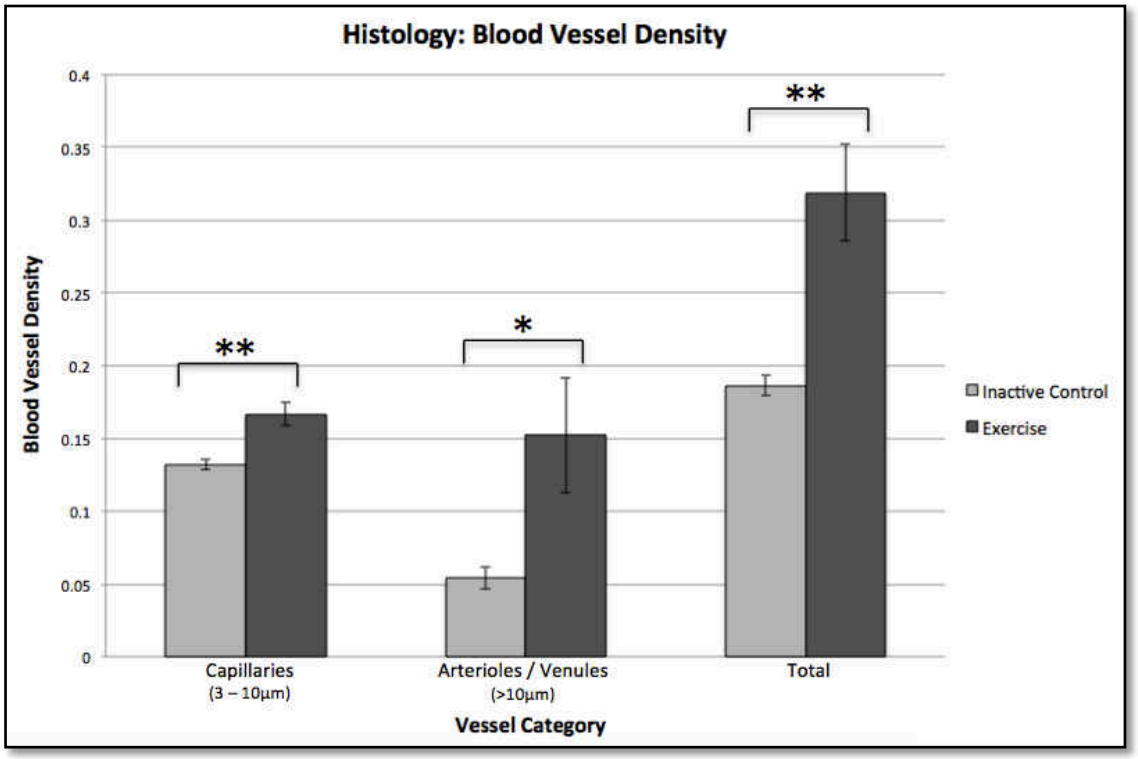

Figure 14. Histology data analyses revealed VX animals had greater blood vessel densities when compared to IC (* $p < .05$; ** $p < .005$)

Additionally, results from an independent-samples t-test indicate a significantly greater ($t_{(12)} = 2.433$, $p = .032$; see *Figure 14*) arteriole/venule density in VX animals ($M = .152$, $SD = .104$) when compared to IC ($M = .054$, $SD = .02$). Similarly, results from an independent-samples t-test revealed a significantly greater ($t_{(12)} = 3.977$, $p = .002$; see *Figure 14*) capillary density in VX animals ($M = .167$, $SD = .021$) when compared to IC ($M = .132$, $SD = .01$).

Histology: Vessel Counts by Size

Due to the unique staining characteristics of the tissue, and the variation in arteriole / venule diameter noted in the previous analysis (>10μm), a size analysis was conducted in order to further examine patterns of angiogenesis. From the images collected, a 20% subsample was employed for this analysis. Within the selected images, each vessel that was counted in the original point grid analysis was traced and its diameter was recorded, producing a total 439 points of interest. From the collected data, the range of diameters was divided into tertiles, producing total vessel counts for each size category.

Paired-samples t-tests indicated a significantly greater number of small vessels ($M = 44.143$, $SD = 29.958$) than medium ($M = 4.286$, $SD = 4.855$) sized vessels within the VX group from the histology images subsampled; $t_{(6)} = 3.982$, $p = .007$; see *Figure 15*. Also, there were significantly more small vessels than large ($M = 0.517$, $SD = 0.787$) sized vessels within VX group from the histology images subsampled; $t_{(6)} = 3.836$, $p = .009$. Similarly, paired-samples t-tests indicated a significantly greater number of small vessels ($M = 13.429$, $SD = 8.304$) than medium ($M = 0.488$, $SD = 0.184$) sized vessels within the IC group from the subsampled histology images; $t_{(6)} = 3.982$, $p = .007$. Likewise, there were significantly more small vessels than large ($M = 0.000$, $SD = 0.000$) sized vessels within IC group from the subsampled histology images; $t_{(6)} = 3.836$, $p = .009$. Furthermore, independent-sample t-tests revealed a greater

number of small vessels in VX animals ($M = 44.143$, $SD = 29.958$) when compared to the small vessel counts of IC ($M = 13.429$, $SD = 8.304$) animals; $t_{(12)} = 2.614$, $p = 023$. Between medium and large sized vessels, there were no statistical differences within-groups, nor where there any statistical between-group differences in these size categories.

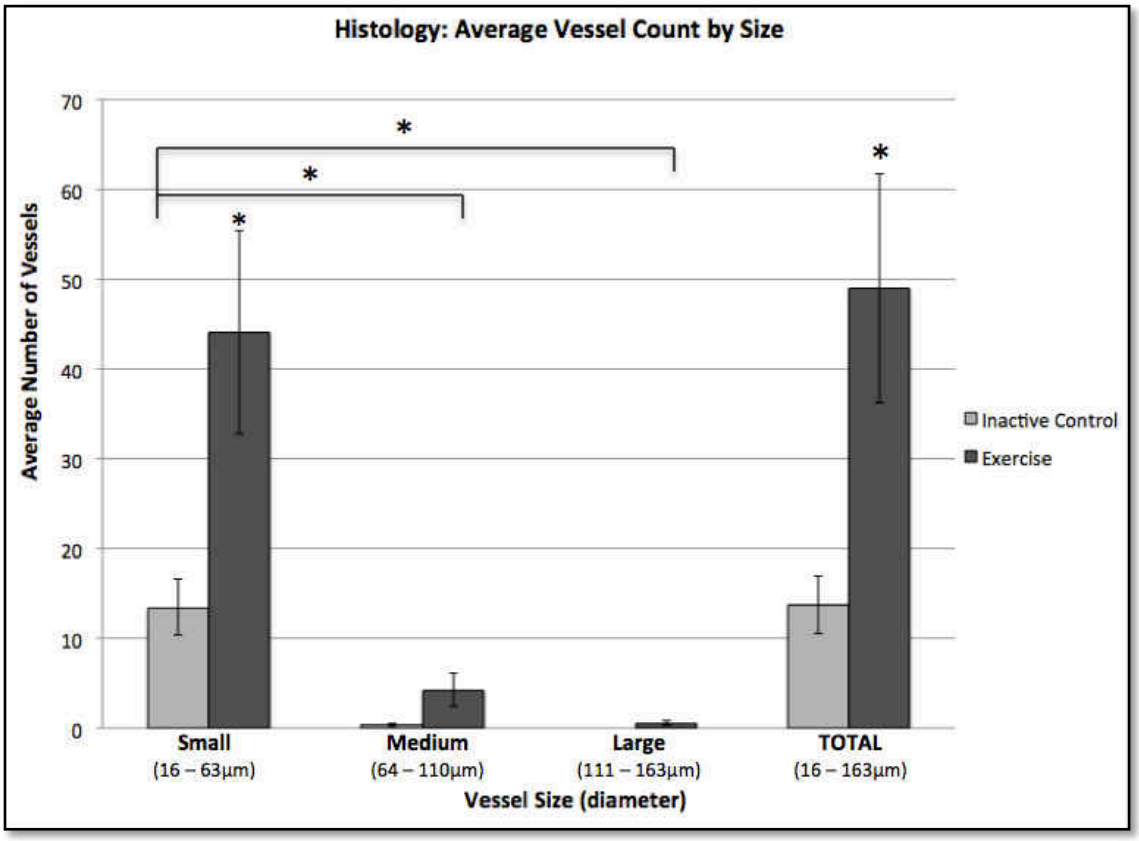

Figure 15. Within the arteriole / venule category of vessels, the smallest in size appear to be driving the observed differences (* $p < 0.05$)

Histology: Small Vessel Size Analysis

To further examine this pattern, the diameter range for the small vessels was again divided into tertile categories. The purpose of this analysis is to demonstrate that it is the smallest of the arterioles / venules driving the observed changes, and that the differences between exercise and inactive control groups are significant. In each of the categories, VX animals had a significantly greater number of vessels when compared to inactive controls. For

both VX and IC groups, the smallest vessels, defined by a diameter range of 16.15µm – 31.82µm, significantly outnumbered vessels in the middle and largest categories (see *Figure 16*).

Results from a paired-samples t-test indicated a significantly greater number of the smallest vessels (M = 27.86, SD = 15.99) than mid-sized small vessels categorized by a diameter of 31.82µm—47.5µm (M = 12.14, SD = 10.78) within the VX group; $t_{(6)} = 6.582$, $p = 0.001$; see *Figure 16*. Also, on average there were significantly more of the smallest vessels than the largest (M = 4.14, SD = 3.98) small vessels observed in the subsample of images from the VX group; $t_{(6)} = 4.931$, $p = 0.003$. In addition, results indicated a significantly greater number of mid-sized small vessels (M = 12.14, SD = 10.78) when compared to the largest of the small vessels categorized by a diameter of 47.5µm—63.18µm (M = 4.14, SD = 3.98) observed in the subsample of VX histology images $t_{(6)} = 2.64$, $p = 0.038$.

Similarly, results from the paired-sample t-tests indicated a significantly greater number of the smallest vessels (M = 10.43, SD = 7.18) than mid-sized small vessels (M = 2.57, SD = 1.27) within the IC group; $t_{(6)} = 3.15$, $p = 0.020$; see *Figure 16*. In addition, on average there were significantly more of the smallest vessels than the largest (M = 0.429, SD = 0.535) small vessels observed in the subsample of images from the IC group; $t_{(6)} = 3.846$, $p = 0.009$. Results also indicated a significantly greater number of mid-sized small vessels (M = 2.57, SD = 1.27) when compared to the largest of the small vessels (M = 0.429, SD = 0.535) observed in the subsample of IC histology images $t_{(6)} = 6.301$, $p = 0.001$.

Lastly, results from an independent-samples t-test indicate a greater number of the smallest vessels in VX animals (M = 27.86, SD = 15.99) when compared to IC (M = 10.43, SD = 7.18) animals; $t_{(12)} = 2.630$, $p = 0.022$, see *Figure 16*. Results also indicated a greater number of the mid-size small vessels in VX animals (M = 12.14, SD = 10.78) when compared to IC (M =

2.57, *SD* = 1.27) animals; $t_{(12)} = 2.334$, $p = 0.038$, and a greater number of the largest of the small vessels in VX (*M* = 4.14, *SD* = 3.98) when compared to IC (*M* = 0.429, *SD* = 0.535) animals; $t_{(12)} = 2.449$, $p = 0.031$, see *Figure 16*.

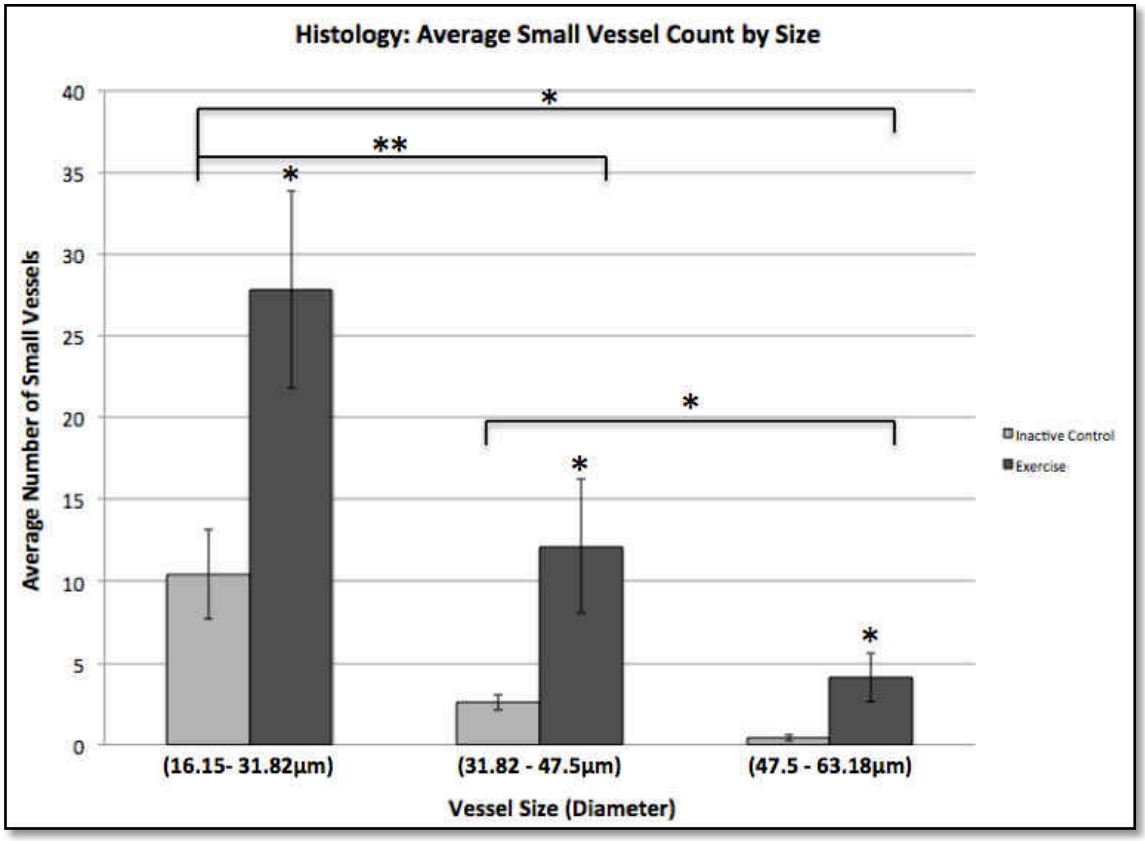

Figure 16. Smallest vessels are greater in number than any other size category. The differences in blood vessel count between VX and IC are significant (* $p < .05$, ** $p < .005$)

DISCUSSION

Study Aims

The purpose of this study was to investigate the utility of Spectral Domain-Optical Coherence Tomography in the examination of cerebrovascular plasticity, as assessed by exercise-induced changes in blood vessel density and hypoxia-induced vasodilation. To validate this novel technique, we sought to compare data captured by SD-OCT with data collected via traditional methods of histology. In the first phase of the experiment, animals were provided

voluntary access to a running wheel for average 26-weeks. In the second phase of the experiment, animals were anesthetized and then exposed to a laboratory-induced condition of hypoxia-hypercapnia while under the lens of the SD-OCT scanner. After scanning was completed animals were sacrificed for histology. Using both techniques, we found that exercised animals had significantly greater total blood vessel densities when compared to inactive controls, suggesting that exercise facilitated the growth of new blood vessels; a finding consistent with numerous other studies (Black et al., 1990, Issacs et al., 1992; Kleim et al., 2002; Swain et al., 2003). Furthermore, the histological analysis of vessels by size indicated a significantly greater number of small vessels in exercised animals when compared to inactive controls. This finding suggests that venulo-arteriogenesis also may have been induced by exercise, and may have contributed to the observed changes within the small vessel category. Moreover, the application of SD-OCT expanded our understanding of exercise-induced cerebrovascular plasticity. Not only did we find a greater average small vessel diameter within exercised animals, which supports our claim for exercise-induced venulo-arteriogenesis, but when oxygen and carbon dioxide gases were manipulated to create a hypoxic-hypercapnic condition, these vessels expanded nearly double the degree to which small vessels in inactive controls did. This suggests that exercise training facilitates cerebrovascular reactivity, or a more adaptive response when oxygen is deprived.

The terminology used within this discussion is important to note. Given that our methods did not allow us to distinguish between arterioles (i.e., small vessels carrying blood from the heart) and venules (i.e., small vessels carrying blood back to the heart), we use the term *small vessels* to more generally describe this size category. Furthermore, the SD-OCT diameter analysis revealed a small percentage (2.67%) of the small vessels sampled measured 3-10μm in

diameter. Thus, within the segment of this discussion including the diameter analysis, it should be noted that capillaries are also described using the term *small vessels.* In addition, the current literature describes continued growth of small vessels more broadly as arteriogenesis. However, despite the lack of empirical evidence, it is equally likely that the same endothelial adaptations that are improving arteriole function are also improving venous circulation. Thus, we use the term venulo-arteriogenesis to more accurately describe our observations.

Interpreting the Results

Blood Vessel Density

Our findings from the SD-OCT data provide strong evidence for exercise-induced changes in blood vessel density. We demonstrated that animals that were provided voluntary access to a running wheel had significantly greater total blood vessel density when compared to inactive controls. Findings from our histological data analyses confirmed this observation.

Angiogenesis (i.e., the growth of new vessels from preexisting capillaries) occurs in several regions of the brain in response to exercise. For example, our findings corroborate one of the earliest investigations conducted by Black and colleagues (1990) who found a significant increase in capillary density of the cerebellar paramedian lobules (i.e., forelimb region of cerebellar cortex) of exercised rats. Another key study investigating the relationship between exercise and cerebellar vasculature was that of Isaacs and colleagues (1992), who found significant reductions in quantified diffusion distances (mean distance to nearest capillary from random point in tissue) in the cerebellar paramedian lobules. Most relevant to our study, other investigations provide compelling evidence to support exercise-induced capillary expansion in the motor cortex. For example, Kleim and colleagues (2002) provided rats with thirty days of free access to a running wheel. Following analyses of the microstimulation map and histology

data, exercised rats were found to have significantly greater capillary density within layer V in the forelimb representation of motor cortex when compared to inactive controls. Similarly, Swain and colleagues (2003) found that voluntary exercise induces concomitant increases in capillary density and cerebral blood volume in the rat motor cortex. Together, these findings support the interpretation of our results.

Our findings for blood vessel density using SD-OCT were unexpected. Only when vessels size categories were combined to total blood vessel density did we see a statistically significant main effect for group. There are a number of possible explanations for this. For one, SD-OCT is limited to a spatial resolution of ~5μm. From the total number of vessels included in the SD-OCT analyses, the smallest diameter recorded was 6.708μm. For comparison, the smallest vessel sampled via traditional methods of histology was 2.963μm. Studies indicate that cerebral capillaries typically range ~3-10μm (Cortés-Sol et al., 2013; Farrell et al., 1987), but generally measure approximately ~5μm in diameter (Duelli & Kuschinsky, 1993; Villringer et al., 1994) under normal oxygen conditions. Thus, it is unlikely SD-OCT was able to capture the same population of capillaries that were successfully sampled via traditional methods of histology. For example, during the vessel diameter analysis, only 2.67% of the vessels sampled fell within the capillary category. In contrast, our histological analyses revealed the greatest density in any size category of vessels were capillaries ranging ~3-10μm in diameter (refer to *Figure 14*). This finding is consistent with what has been established in the literature. That is, capillary density is greatest, particularly in brain regions with the highest synaptic density and metabolic demand (Klein et al., 1986; Macdonald et al., 2009). As previous studies have demonstrated, it is possible to observe exercise-induced angiogenesis with traditional histology. A similar observation using SD-OCT is feasible, yet more challenging.

Another plausible explanation of our SD-OCT findings relates yet again to the technical capacity of the device. When projected light from the scanning device contacts moving blood particles in the tissue, it is then deflected. Some of this light is reflected back to the lens of the SD-OCT device and is recorded. However, the reflection of light upon contact with moving particles inhibits observations beyond this point of contact. In other words, it is not possible to collect data beyond a vessel that has been imaged. Even shifting the focal point of the lens will not resolve this problem, as any vessel with moving blood particles would cast a shadow on the tissue beneath it. Thus, imaging large vessels in external cortical layers inhibits the observation of smaller vessels in deeper layers of cortex. Given what we know about the robust exercise-induced growth of capillaries in layer V of M1 (Kleim et al., 2002), this is problematic, and likely why we did not see statistical differences between groups with the SD-OCT data when vessel size categories were analyzed independently.

Our findings from the histological size analyses were also interesting. Results not only indicated a statistically greater number of small vessels than any other size category, but a significantly greater number of small vessels (i.e., arterioles) in exercised rats when compared to inactive controls. When parsed out further, a pattern emerged. In each analysis, the smallest vessels consistently outnumber larger size categories. Additionally, exercised rats displayed greater small vessel counts when compared to inactive controls. This pattern in combination with data collected from the exercise group's running behavior indicates that venulo-arteriogenesis may be an underlying factor for these observed differences.

Unlike the sprouting of a new vessel during angiogenesis, venulo-arteriogenesis is the continued growth of an existing vessel, such that the vessel's diameter expands to allow for a greater volume of blood to reach tissue. Research indicates that venulo-arteriogenesis is induced

by increased flow demands and altered shear stress on the vascular wall (i.e., the variable force exerted by the changing intravascular blood flow rate). In the laboratory, venulo-arteriogenesis is often surgically stimulated by manipulating flow demands within major arteries of the rat brain. The vascular systems of the body, including those within the brain, contain protective collateral systems that are able to compensate for disruptions in blood supply by restoring flow in vessels that remain unobstructed. Within the brain, the circle of Willis is the central collateral system that connects four primary supplying arteries: both pairs of carotid and vertebral arteries. Typically, a combination of ligatures and arteriovenous shunts are used to alter blood flow in non-occluded arteries. For example, in a study conducted by Busch and colleagues (2003), a three-vessel occlusion (unilateral common carotid artery occlusion in combination with bilateral vertebral artery occlusion) was employed to induce venulo-arteriogenesis within the circle of Willis in adult rats. The other free-flowing arteries of the brain were burdened with restoring hemodynamic homeostasis. As a result, arteriole diameter within the posterior cerebral artery ipsilateral to the carotid occlusion increased significantly within one week, and the posterior cerebral artery contralateral to the occluded carotid artery significantly increased its diameter within three weeks. To build upon this finding, Schierling and colleagues (2009) utilized comparable combinations of ligatures and shunts to increase cerebral collateral circulation and fluid shear stress. Similarly, increases in blood flow correlated with increases in diameter and length of the nonligated arterioles.

Increased blood flow is directly related to the force exerted on the endothelial wall of the vessel, and these physiological stimuli trigger many of the same mechanisms that prompt angiogenesis (Schaper, 2009). Adhesion molecules, such as intracellular adhesion molecule (CD54), and a host of growth factors, such as fibroblast growth factors (FGFs) and vascular

endothelial growth factor (VEGF) facilitate endothelial and smooth muscle cell proliferation (Heil & Schaper, 2004; Schaper, 2009). Furthermore, as we have briefly discussed, exercise induces an increase in cerebral blood flow in several regions of the brain (Delp et al., 2001; Thomas et al., 2012), including motor cortex (Swain et al., 2003). Although there are other factors that influence hemodynamic shear stress (e.g., vessel geometry, fluid viscosity), increased intravascular blood flow is a potent stimulus for adaptive modifications of the vessel wall (Schaper, 2009). Taken together, this evidence supports our claim that an exercise-induced state of hypoxia can stimulate venulo-arteriogenesis, as it does angiogenesis.

Several investigations have explored the relationship between exercise and angiogenesis. In such studies, animals are often provided with access to a running wheel for approximately thirty days (Black et al., 1990, Issacs et al., 1992; Kleim et al., 2002; Swain et al., 2003), and results consistently indicate significantly greater capillary density when compared to inactive controls. It is likely that these significant differences are induced by the animal's rapid increase in running behavior over this 4-week time period (refer to *Figure 11)*. While we did not collect data at that time point, it is very likely we would have seen similar results. However, the fact that the animals in this study were provided access to a running wheel for much longer than thirty days allows us to speculate the influence of chronic exercise on the cerebrovascular system. Given that exercise causes a state of mild hypoxia in the brain (Berggren et al., *in preparation*) and increases cerebral blood flow (Swain et al., 2003), it is highly likely that the animal's chronic exposure to exercise in this study induced a state of hemodynamic shear stress. Over time, the cerebrovascular system adapted to allow for greater volumes of oxygen rich blood to reach brain tissue in the primary motor cortex.

An additional aim of this study was to capture Doppler flowmetry data in order to further address this concept. We had expected to see greater blood perfusion in exercised animals when compared to inactive controls. Unfortunately, the data collected via SD-OCT Doppler was not suitable for analysis. In brief, inflammation within the scanned region of interest likely inhibited the collection of usable data. A more detailed explanation can be found in the subsequent *Limitations* section of this discussion.

Despite the lack of Doppler data to support this finding, a diameter analysis of the SD-OCT imaged vessels indicates that smaller vessels have the capacity to adapt to phasic increases in cerebral blood flow induced by exercise. Our finding that small vessel diameter of exercised rats was significantly larger in both baseline and hypoxic conditions when compared to inactive controls suggests that many of the same mechanisms that induce the growth of new capillaries, may also facilitate the growth of existing arterioles. This finding is supported by a previous study conducted by Patt and colleagues (1997), who found significantly larger average blood vessel size in animals exposed to 30 days of incremental reductions in oxygen availability when compared to normoxia exposed controls. The temporal pattern of vascular growth (i.e., the formation of new vessels, and continued growth of existing vessels) is still largely unknown.

Blood Vessel Dilation

Our findings from the SD-OCT data provide strong evidence for exercise-induced changes in cerebrovascular reactivity. When compared to inactive controls, we demonstrated that animals that were provided voluntary access to a running wheel exhibited a significantly greater degree of small vessel dilation when oxygen and carbon dioxide levels were manipulated. This finding suggests that the cerebrovascular system within motor cortex of exercised rats was better able to adapt to the condition of hypoxic-hypercapnic stress.

Cerebrovascular reactivity (CVR) is the change in intravascular flow rate following some vasoactive stimuli and reflects the capacity to which vessels dilate (Thrippleton, 2015; Yezhuvath et al., 2009). For example, when oxygen demand increases during exercise, a host of molecular signals (e.g., eNOS, HIFs, etc.) induce a cascade of mechanisms (e.g., PI3K/Akt signaling, PLC- γ signaling) that regulate the dilation of blood vessels via several molecular pathways (Karar & Maity, 2011; Dudzinski & Michel, 2007). Vasodilation in response to hypoxia allows more glucose rich hemoglobin to reach cell tissue; thereby, restoring hemodynamic homeostasis.

Our finding that small vessels of exercised animals dilate to a significantly greater degree (~two-fold on average) when compared to inactive control animals is interesting. This finding suggests that exercise training likely promotes the endothelial adaptation of what we have termed, *vasoflexibility*. That is, exercise training conditioned the vessels of the forelimb representation in motor cortex to enable a greater capacity to dilate, which theoretically facilitated greater volumes of oxygen rich blood to reach tissue under the laboratory-induced conditions of oxygen deprivation. Ideally, we would have confirmed this finding using SD-OCT Doppler. Unfortunately, as is described in greater detail within the *Limitations* section of this discussion, we were unable to collect Doppler data suitable for analysis. Despite the lack of Doppler data to support this finding, the diameter analysis of the SD-OCT imaged vessels indicates that smaller vessels have the capacity to adapt to the phasic increases in cerebral blood flow and vascular shear stress associated with hypoxia.

Although the mechanisms underlying the vasoprotective effects of exercise are largely unknown, there is compelling evidence that many of the same factors driving angiogenesis and venulo-arteriogenesis are involved in the endothelial adaptations that lead to greater

vasoflexibility. As previously discussed, exercise-induced endothelial adaptations are largely driven by the repeated episodes of increased intravascular flow and shear stress on the endothelial wall (Green, 2009; Jasperse & Laughlin, 2006). It is also likely that the circulating factors, such as eNOS and VEGF, described previously in the discussion of vasodilation signaling pathways play an important role in vascular remodeling (Papapetropoulos et al., 1997; Rudic et al., 1998; Murohara et al., 1998; Heil & Schaper, 2004; Schaper, 2009) and vasoprotection (Endres et al., 2003; Gertz et al., 2006; Mayhan et al., 2010). Furthermore, the repeated exposure to mild conditions of hypoxia may strengthen the cerebrovascular system such that it becomes more resistant to hypoxic threat. In a study conducted by Dunn and colleagues (2013), hypoxic pre-conditioned rats were found to have a significant reduction in inflammatory markers and infarct volume 48 hours post-MCA occlusion.

In sum, the studies presented herein provide evidence that exercise induces a number of vasoprotective adaptations. The interplay of factors underlying vascular remodeling and vasoprotection is largely unknown, but the increase in cerebral blood flow during phases of exercise should be considered a key component and continue to be investigated. Various techniques can be employed to do so. In this study, we have successfully demonstrated that SD-OCT can be utilized to assess cerebrovascular plasticity. Using SD-OCT to capture real-time angioarchitecture, we were successfully able to demonstrate that exercise induces angiogenesis. Although, in comparison, the histology data revealed similar results, yet to a greater degree of sensitivity (i.e., capillaries were accounted for). However, SD-OCT exceeded the utility of histological methods in the investigation of blood vessel dilation. In this study, using SD-OCT, we were able to successfully demonstrate that similar factors driving angiogenesis and venulo-

arteriogenesis may also be involved in the endothelial adaptations that lead to greater vasoflexibility.

Limitations

There were important limitations with this study to note. The craniotomy and durotomy procedures were necessary to produce the highest quality angiograms; however, the removal of the skull and underlying *dura mater* raised significant issues. The resulting inflammation was unpreventable. Throughout the duration of the scanning procedures, variable swelling within the scanned region of interest likely changed the focal plane of the lens. In addition, it is possible the inflammation slightly shifted the geometry of underlying vessels. Doppler is particularly sensitive to changes in the angle of a vessel and any shift in the angle of a vessel compromises the validity of collected data. Doppler spatial resolution is limited to ~20μm. Furthermore, Doppler measures axial velocity and is thereby limited to collecting hemodynamic data from vessels with some angle relative to the perpendicular plane of the scanning lens and projected waves of light. The craniotomy-durotomy procedure and the resulting accumulation of blood created another problem for Doppler, and similarly for OCT angiography. Two animals expired during surgery due to incessant bleeding around the scanned region of interest. Furthermore, for optimal recording, the lens is fixed approximately 2mm above the tissue intended for scanning. The close proximity of the lens to tissue did not allow us to remove accumulating blood without adjusting the position of the scanning lens. Once moved, we were challenged with returning the lens to the exact position before initiating subsequent scans. During the analysis of vessel diameter, we controlled for this issue by storing measurements in the 'ROI Manager' of the ImageJ software. By doing so, we were able to ensure that the same segment of each vessel measured in the baseline angiogram, was also measured in the hypoxia angiogram.

An additional limitation to this study was the gas mixture chosen to induce hypoxia-hypercapnia. In total, three animals expired during the hypoxia scanning session. Therefore, we suggest that the 10% oxygen and 5% carbon dioxide mixture was likely too strenuous for some animals while under anesthesia. It should be noted that the three animals that expired during hypoxia were also under anesthesia for a slightly longer duration than others. This was due to excessive bleeding around the scanned region of interest. A combination of Gelfoam sponge, Actel hemostatic gauze, and dental wax was necessary for bleeding to subside. However, these additional steps were time consuming and the lengthy duration in which these animals were under anesthesia may have heightened their sensitivity to hypoxic-hypercapnic threat.

General Conclusions & Future Directions

In conclusion, this thesis demonstrates that Spectral Domain-Optical Coherence Tomography can be utilized to successfully examine cerebrovascular plasticity. We have shown that SD-OCT can detect general changes in blood vessel density, and have confirmed this finding by comparing data with that of traditional histological methods. In addition, SD-OCT expanded our understanding of vasoprotective adaptations by probing beyond what is possible using traditional methods of histology. Using SD-OCT, we not only demonstrated the capacity to visualize angioarchitecture, but the functional capacity to capture real-time cerebrovascular reactivity and vasoflexibility. Furthermore, this thesis makes a significant contribution to the field by expanding what is known about angiogenic and vasoprotective adaptations. Exercise-induced endothelial adaptations (e.g., structural and dilatory) ensure optimal use of the cerebrovascular system. In other words, exercise training conditions the cerebrovascular system such that it is less susceptible to hypoxic stress.

The current research has practical applications in both research and clinical settings. Given that exercise has been shown to improve cognitive performance in animal and human populations (Erickson et al., 2011; Hillman et al., 2006; Hillman, Erickson, & Kramer, 2009; Hogan, Mata, & Carstensen, 2013), one interesting study design using SD-OCT would be to map the temporal progression of cerebrovascular adaptations (e.g., angiogenesis, venulo-arteriogenesis, vasoflexibility) while concomitantly testing improvements in cognitive function. This could be made possible by implanting a cerebral window over the scanned region of interest to enable scanning at any time point before, during, or following exercise intervention. In addition, animals could be subjected to various learning and memory paradigms (e.g., Morris Water Maze) throughout the duration of exercise engagement.

Additionally, there is considerable interest in the adaptive cerebrovascular mechanisms triggered by exercise, particularly as they relate to brain injury and recovery (Arai et al., 2009; Cobianchi et al., 2016; Ding et al., 2004; Larpthaveesarp et al., 2015; Zhang et al., 2013). Our findings contribute to this interest by identifying a number of endothelial-mediated adaptations induced by exercise. With this knowledge, future investigations could utilize SD-OCT with other technologies (e.g., MRI, two-photon microscopy) to explore how these exercise-induced adaptations protect the brain from ischemic insult and aid recovery post-injury. A particularly interesting study would be to address the question: can exercise facilitate recovery following ischemic insult? In such a study, SD-OCT could be utilized to explore the effects of exercise training on stroke recovery by mapping the rate of re-vascularization of the infarct area in exercised animals and non-exercised controls. In addition, it would be interesting to explore the effects of exercise on the cerebrovascular system within the *penumbra*.

Although our SD-OCT findings shed light on the cerebrovascular adaptations induced by exercise, a number of questions remain. One important question of considerable debate within the literature: do brain capillaries (3-10μm) increase in diameter as oxygen demand increases? It should be noted that capillaries are comprised of a single layer of endothelial cells connected at tight junctions, and unlike larger vessels (e.g., arterioles), capillaries are not wrapped with smooth muscle cells (Ballabh, Braun, & Nedergaard, 2004). Thus, their capacity to expand is limited. In addition, the *basal lamina* (i.e., layer of extracellular matrix that forms the surface for which endothelial cells are situated) is densely composed of collagens (e.g., type IV) relative to elastin (Shamloo et al., 2015; Wang-Fischer & Koetzner, 2009), which produces a more rigid structure important in the regulation of the blood-brain-barrier. However, the evidence supporting the important role of pericytes in cerebral capillary activity (Bergers & Song, 2005; Hall et al., 2014) may indicate some room for flexibility. Pericytes are small vascular cells that regulate contractility of the microvasculature, endothelial cell activity, and macrophage function (Rucker, Wynder, & Thomas, 2000). Similar to the smooth muscle function in larger vessels, pericytes can stimulate vasoconstriction and vasodilation within the capillary beds (i.e., network of capillaries) to produce changes in vessel diameter and capillary blood flow (Rucker, Wynder, & Thomas, 2000). While it is common knowledge that capillaries do not mechanically dilate in the same manner arterioles do, the binding of vasoactive signals to endothelial cells and subjacent pericytes may allow for some limited expansion during the neurovascular exchange of glucose, oxygen, and other important factors. In one particular study, Villringer and colleagues (1994) found that capillary diameter increased significantly (.33 microns on average) in response to hypercapnic stimulation. This finding indicates that the regulation of capillary blood flow is, at least in part, mediated by changes in capillary diameter. Taken together, the presented

evidence indicates that capillaries have limited capacity to expand, but may do so in response to increased neuronal activity and metabolic demand (Hamilton, Attwell, & Hall, 2010; Stefanovic et al., 2007), most likely to facilitate the rapid transport of oxygen rich red blood cells to tissue (Hutchinson et al., 2006; Itoh & Suzuki, 2012).

Another important question to consider addresses the rate in which the previously described endothelial-mediated adaptations occur. That is, what is the timeline for angiogenesis, venulo-arteriogenesis, and vasoflexibility? To date, no single study has explored the temporal sequence for each adaptation as they relate to one another. However, the evidence supporting the driving factors and molecular signals that regulate these phenomena may shed some light on the matter. There are similarities and differences. For example, molecular signals that prompt the rapid dilation of vessels (e.g., eNOS signaling via HIF-1α) also stimulate the growth of new ones (e.g., VEGF via HIF-1α). The transcription factor HIF-1α has been found to increase immediately in response to a single bout of exercise (Berggren et al., in preparation). Thus, the driving factor for angiogenesis is hypoxia. In contrast, venulo-arteriogenesis is stimulated by chronic vascular shear stress as a result of increased blood flow, as is likely the case for vasoflexibility. The increased tension on the vascular wall signals a cascade of mechanisms that recruit circulating monocytes via monocyte chemoattractant protein-1 (MCP-1) and induce endothelial proliferation via growth factors, like granulocyte macrophage colony-stimulating factor (GM-CSF). Although both angiogenesis and venulo-arteriogenesis serve to restore disruptions in vascular circulation, the current evidence indicates that angiogenesis (i.e., new vascular growth) can occur within days (Baluk et al., 2004; Hathout et al., 2009; Kerr & Swain, 2011; Van der Borght et al., 2009; Zhu et al., 2015), whereas arteriogenesis (i.e., vascular remodeling) occurs within several days to weeks (Busch et al., 2003; Helisch et al., 2005; Hoefer

et al., 2001; Leong-Poi et al., 2005). Furthermore, vasoflexibility likely mirrors changes in arteriole remodeling. As endothelial cells proliferate, smooth muscle cells synthesize new elastin (Scholz et al., 2000); thus, creating a more flexible vascular unit. Given what has been established within the literature, we speculate that angiogenesis occurs rather rapidly, and is followed by arteriogenesis, which corresponds with the improved flexibility of the cerebrovascular system. However, further investigation is necessary to fully understand the temporal pattern in which these events occur.

REFERENCES

Ameln, H., Gustafsson, T., Sundberg, C. J., Okamoto, K., Jansson, E., Poellinger, L., & Makino, Y. (2005). Physiological activation of hypoxia inducible factor-1 in human skeletal muscle. *Federation of American Societies for Experimental Biology Journal, 19*(8), 1009-1011.

Anderson, B. (2002). Alterations in the thickness of motor cortical subregions after motor-skill learning and exercise. *Learning & Memory, 9*(1), 1-9.

Arai, K., Jin, G., Navaratna, D., & Lo, E. H. (2009). Brain angiogenesis in developmental and pathological processes: Neurovascular injury and angiogenic recovery after stroke. *FEBS Journal, 276*(17), 4644-4652.

Atry, F., Frye S., Richner, T., Brodnick, S., Soehartono, A., Williams, J., & Pashaie, R. (2014). Monitoring of cerebral hemodynamics post optogenetic stimulation via optical coherence tomography. *IEEE Transactions on Bio-medical Engineering, 62*(2), 766-773.

Ballabh, P., Braun, A., & Nedergaard, M. (2004). The blood–brain barrier: An overview: Structure, regulation, and clinical implications. *Neurobiology of Disease 16*(1), 1-13.

Baluk, P., Lee, C. G., Link, H., Ator, E., Haskell, A., Elias, J. A., & Mcdonald, D. M. (2004). Regulated angiogenesis and vascular regression in mice overexpressing vascular endothelial growth factor in airways. *The American Journal of Pathology, 165*(4), 1071-1085.

Bergers, G., & Song, S. (2005). The role of pericytes in blood-vessel formation and maintenance. *Neuro-Oncology, 7*(4), 452-464.

Berggren, K.L., Ahuja, B.A., Kay, J.J.M., Pochinski, B., & Swain, R.A. (in preparation). Treadmill exercise rapidly induces the expression of HIF-1α in the hippocampus of the adult rat.

Berggren, K.L., Kay, J.J., & Swain, R.A. (2014). Examining cerebral angiogenesis in response to physical exercise. *Methods in Molecular Biology, 1135*, 139-154.

Black, J.E., Isaacs, K.R., Anderson, B.J., Alcantara, A.A., & Greenough, W.T. (1990). Learning causes synaptogenesis, whereas motor activity causes angiogenesis, in cerebellar cortex of adult rats. *Proceedings of the National Academy of Sciences of the United States of America, 87*(14), 5568-72.

Boppart, S. (2015). Biophotonics Imaging Laboratory. Retrieved April 05, 2016, from http://biophotonics.illinois.edu/technology/oct/

Bullitt, E., Rahman, F.N., Smith, J.K., Kim, E., Zeng, D., Katz, L.M., & Marks, B.L. (2009). The effect of exercise on the cerebral vasculature of healthy aged subjects as visualized by MR angiography. *American Journal of Neuroradiology, 30*(10), 1857-63.

Busch, H., Buschmann, I. R., Mies, G., Bode, C., & Hossmann, K. (2003). Arteriogenesis in hypoperfused rat brain. *Journal of Cerebral Blood Flow & Metabolism, 23*, 621-628.

Chae, C., & Kim, H. (2009). Forced, moderate-intensity treadmill exercise suppresses apoptosis by increasing the level of NGF and stimulating phosphatidylinositol 3-kinase signaling in the hippocampus of induced aging rats. *Neurochemistry International, 55*, 208-213.

Chen, T. (2005). Spectral domain optical coherence tomography: Ultra-high speed, ultra-high resolution ophthalmic imaging. *Archives of Ophthalmology, 123*(12), 1715-1720.

Chen, J., Venkat, P., Zacharek, A., & Chopp, M. (2014). Neurorestorative therapy for stroke. *Frontiers in Human Neuroscience, 8*, 382.

Cines, D.B., Pollak, E.S., Buck C.A., Loscalzo, J., Zimmerman, G.A., McEver, R.P., Pober, J.S., Wick, T.M., Konkle, B.A., Schwartz, B.S., Barnathan, E.S., McCrae, K.R., Hug, B.A., Schmidt, A-M., & Stern, D.M. (1998). Endothelial cells in physiology and in the pathophysiology of vascular disorders. *Blood, 91*(10), 3527-3561.

Cipolla, M.J. (2009). Control of Cerebral Blood Flow. In The Cerebral Circulation. San Rafael (CA): Morgan & Claypool Life Sciences, p. 29-38.

Cobianchi, S., Arbat-Plana, A., López-Álvarez, V., & Navarro, X. (2016). Neuroprotective effects of exercise treatments after injury: The dual role of neurotrophic factors. *Current Neuropharmacology, 14*(999), 1-1.

Cooley, J.W., & Tukey, J.W. (1965). An algorithm for the machine calculation of complex Fourier series. *Mathematics of Computation, 19*(90), 297-302.

Cortés-Sol, A., Lara-Garcia, M., Alvarado, M., Hudson, R., Berbel, P., & Pacheco, P. (2013). Inner capillary diameter of hypothalamic paraventricular nucleus of female rat increases during lactation. *BioMed Central Neuroscience, 14*(7), 1-8.

Cui, X., Chopp, M., Zacharek, A., Zhang, C., Roberts, C., & Chen, J. (2009). Role of endothelial nitric oxide synthetase in arteriogenesis after stroke in mice. *Neuroscience, 159*, 744–750.

Delp, M. D., Armstrong, R. B., Godfrey, D. A., Laughlin, M. H., Ross, C. D., & Wilkerson, M. K. (2001). Exercise increases blood flow to locomotor, vestibular, cardiorespiratory and visual regions of the brain in miniature swine. *The Journal of Physiology, 533*(3), 849-859.

Ding, Y., Luan, X., Li, J., Rafols, J., Guthinkonda, M., Diaz, F., & Ding, Y. (2004). Exercise-induced overexpression of angiogenic factors and reduction of ischemia/reperfusion injury in stroke. *Current Neurovascular Research, 1*(5), 411-420.

Donoghue, J., Suner, S., & Sanes, J. (1990). Dynamic organization of primary motor cortex output to target muscles in adult rats II. Rapid reorganization following motor nerve lesions. *Experimental Brain Research, 79*, 492-503.

Donoghue, J.P., Wise, S.P., (1982). The motor cortex of the rat: Cytoarchitecture and microstimulation mapping. *The Journal of Comparative Neurology, 212*, 76-88.

Dudzinski, D., & Michel, T. (2007). Life history of eNOS: Partners and pathways. *Cardiovascular Research, 75*(2), 247-260.

Duelli, R., & Kuschinsky, W. (1993). Changes in brain capillary diameter during hypocapnia and hypercapnia. *Journal of Cerebral Blood Flow & Metabolism, 13*(6), 1025-1028.

Dugdale, D. (2012, August 29). Cerebral hypoxia: MedlinePlus Medical Encyclopedia (D. Zieve, Ed.). Retrieved February 3, 2015, from: http://www.nlm.nih.gov/medlineplus/ency/article/001435.htm

Dunn, J.F., Wu, Y., Zhao, Z., Srinivasan, S., & Natah, S.S. (2013). Training the brain to survive stroke. *Public Library of Science One, 7*(9): e45108

Endres, M., Gertz, K., Lindauer, U., Katchanov, J., Schultze, J., Schrock, H., Nickenig, G., Kuschinsky, W., Dirnagl, U., & Laufs, U. (2003). Mechanisms of stroke protection by physical activity. *Annals of Neurology, 54*(5), 582–590.

Erickson, K. I., Voss, M.W., Prakash, R. S., Basak, C., Szabo, A., Chaddock, L., Kim, J., Heob, S., Alves, H., White, S.M., Wojcicki, T.R., Mailey, E., Vieira, V.J., Martin, S.A., Pence,

B.D., Woods, J.A., McAuley, E., & Kramer, A.F. (2011). Exercise training increases size of hippocampus and improves memory. *PNAS, 108*(7), 3017-3022.

Farrell, C.R., Stewart, P.A., Farrell, C.L., & Del Maestro, R.F. (1987). Pericytes in human cerebral microvasculature. *Anatomy & Physiology: The Anatomical Record, 218*(4), 466-469.

Fawcett, J. W., Rosser, A. E., & Dunnett, S. B. (2001). Brain Damage, Brain Repair. New York: Oxford University Press.

Fujimoto, J.G. (2003). Optical coherence tomography for ultrahigh resolution in vivo imaging. *Nature Biotechnology, 21*(11), 1361-7.

Fong, G.H., Rossant, J., Gertsenstein, M., & Breitman, M.L. (1995). Role of the Flt-1 receptor tyrosine kinase in regulating the assembly of vascular endothelium. *Nature, 376*(6535), 66-70.

Font, M.A., Arboix, A., & Krupinski, J. (2010). Angiogenesis, neurogenesis, and neuroplasticity in ischemic stroke. *Current Cardiology Reviews, 6*(3), 238-244.

Gale, N., & Yancopoulos, G. (1999). Growth factors acting via endothelial cell-specific receptor tyrosine kinases: VEGFs, Angiopoietins, and ephrins in vascular development. *Genes & Development, 13*(9), 1055-1066.

Gertz, K., Priller, J., Kronenberg, G., Fink, K.B., Winter, B., Schrock, H., Ji, S., Milosevic, M., Harms, C., Bohm, M., Dirnagl, U., Laufs, U., Endres, M. (2006). Physical activity improves long-term stroke outcome via endothelial nitric oxide synthase-dependent augmentation of neovascularization and cerebral blood flow. *Circulation Research, 99*(10), 1132–1140.

Gómez-Pinilla, F., Dao, L., & So, V. (1997). Physical exercise induces FGF-2 and its mRNA in the hippocampus. *Brain Research, 764*(1-2), 1-8.

Granger, D., & Kubes, P. (1996). Nitric oxide as antiinflammatory agent. *Methods in Enzymology, 269*, 434-442.

Green, D.J. (2009). Exercise training as vascular medicine: direct impacts on the vasculature in humans. *Exercise and Sport Sciences Reviews, 37*(4), 196–202

Griesbach, G. S., Hovda, D. A., & Gomez-Pinilla, F. (2009). Exercise-induced improvement in cognitive performance after traumatic brain-injury in rats is dependent upon BDNF activation. *Brain Research, 1288*, 105-115.

Hall, C. N., Reynell, C., Gesslein, B., Hamilton, N. B., Mishra, A., Sutherland, B. A., . . . Attwell, D. (2014). Capillary pericytes regulate cerebral blood flow in health and disease. *Nature, 508*(7494), 55-60.

Hamer, J., Wiedemann, K., Berlet, H., Weinhardt, F., & Hoyer, S. (1978). Cerebral glucose and energy metabolism, cerebral oxygen consumption, and blood flow in arterial hypoxaemia. *Acta Neurochirurgica, 44*(3-4), 151-160.

Hamilton, N. B., Attwell, D., & Hall, C. N. (2010). Pericyte-mediated regulation of capillary diameter: A component of neurovascular coupling in health and disease. *Frontiers in Neuroenergetics, 2*(5), 1-14.

Harten, S. K., Ashcroft, M., & Maxwell, P. H. (2010). Prolyl hydroxylase domain inhibitors: A route to HIF activation and neuroprotection. *Antioxidants & Redox Signaling, 12*(4), 459-480.

Hathout, E., Chan, N. K., Tan, A., Sakata, N., Mace, J., Pearce, W., . . . Obenaus, A. (2009). In vivo imaging demonstrates a time-line for new vessel formation in islet transplantation. *Pediatric Transplantation, 13*(7), 892-897.

Heil, M., & Schaper, W. (2004). Influence of Mechanical, Cellular, and Molecular Factors on Collateral Artery Growth (Arteriogenesis). *Circulation Research, 95*(5), 449-458.

Helisch, A., Wagner, S., Khan, N., Drinane, M., Wolfram, S., Heil, M., Ziegelhoeffer, T., Brandt, U…Schaper, W. (2006). Impact of mouse strain differences in innate hindlimb collateral vasculature. *Arteriosclerosis, Thrombosis, and Vascular Biology, 26*(3), 520-526.

Hillman, C., Erickson, K., & Kramer, A. (2009). Be smart, exercise your heart: Exercise effects on brain and cognition. *Nature Reviews Neuroscience, 9*, 58-65.

Hillman, C. H., Motl, R. W., Pontifex, M. B., Posthuma, D., Stubbe, J. H., Boomsma, D. I., & de Gues, E. J. C. (2006). Physical activity and cognitive function in a crosssection of younger and older community-dwelling individuals. *Health Psychology, 25*(6), 678-687.

Hoeben, A., Landuyt, B., Highley, M.S., Wildiers, H., van Oosterom, A.T., & de Bruijn, E.A. (2004). *Vascular Endothelial Growth Factor and Angiogenesis. Pharmacological Reviews, 56*(4), 549-580.

Hoefer, I., Van Royen, N., Buschmann, I. R., Piek, J. J., & Schaper, W. (2001). Time course of arteriogenesis following femoral artery occlusion in the rabbit. *Cardiovascular Research, 49*(3), 609-617.

Hogan, C., Mata, J., & Carstensen, L. (2013). Exercise holds immediate benefits for affect and cognition in younger and older adults. *Psychology and Aging, 28*(2), 587-594.

Hoier, B., & Hellsten, Y. (2014). Exercise-induced capillary growth in human skeletal muscle and the dynamics of VEGF. *Microcirculation, 21*(4), 301-314.

Huntley, G.W. (1997). Differential effects of abnormal tactile experience on shaping representation patterns in developing and adult motor cortex. *The Journal of Neuroscience, 17*(23), 9220-9232.

Hutchinson, E. B., Stefanovic, B., Koretsky, A. P., & Silva, A. C. (2006). Spatial flow-volume dissociation of the cerebral microcirculatory response to mild hypercapnia. *NeuroImage, 32*(2), 520-530.

Itoh, Y., & Suzuki, N. (2012). Control of brain capillary blood flow. *Journal of Cerebral Blood Flow & Metabolism, 32*(7), 1167-1176.

Jacobs, K., & Donoghue, J. (1991). Reshaping the cortical motor map by unmasking latent intracortical connections. *Science, 251*(4996) 944-947.

Jasperse, J.L., & Laughlin, M.H. (2006). Endothelial function and exercise training: evidence from studies using animal models. *Medicine and Science in Sports and Exercise, 38*(3), 445–454.

Karar, J., & Maity, A. (2011). PI3K/AKT/mTOR pathway in angiogenesis. *Frontiers in Molecular Neuroscience, 4*, 51.

Kerr, A.L., Steuer, E.L., Pochtarev, V., & Swain, R.A. (2010). Angiogenesis but not neurogenesis is critical for learning and memory acquisition. *Neuroscience, 171*(1), 214-226.

Kerr, A.L., & Swain, R.A. (2011). Rapid cellular genesis and apoptosis: effects of exercise in the adult rat. *Behavioral Neuroscience, 125*(1), 1-9.

Kim, B.K., Shin, M.S., Kim, C.J., Baek, S.B., Ko, Y.C., & Kim, Y.P. (2014). Treadmill exercise improves short-term memory by enhancing neurogenesis in amyloid beta-induced Alzheimer disease rats. *Journal of Exercise Rehabilitation, 10*(1), 2-8.

Kim, S. E., Ko, I., Kim, B. K., Shin, M., Cho, S., Kim, C. G., Kim, S.H., Baek, S.S., Lee, E.K., & Jee, Y. (2010). Treadmill exercise prevents aging-induced failure of memory through an increase in neurogenesis and suppression of apoptosis in rat hippocampus. *Experimental Gerontology, 45*, 357-365.

Kimura, H., Weisz, A., Kurashima, Y., Hashimoto, K., Ogura, T., D'Acquisto, F., Addeo, R., Makuuchi, M., & Esumi, H. (2000). Hypoxia response element of the human vascular endothelial growth factor gene mediates transcriptional regulation by nitric oxide: control of hypoxia-inducible factor-1 activity by nitric oxide. *Blood, 95*(1), 189-197.

Kleim, J., Cooper, N., & Vandenberg, P. (2002). Exercise induces angiogenesis but does not alter movement representations within rat motor cortex. *Brain Research, 934*(1), 1-6.

Klein, B., Kuschinsky, W., Schrock, H., & Vetterlein, F. (1986). Interdependency of local capillary density, blood flow, and metabolism in rat brains. *Heart and Circulatory Physiology, 251*(6), 1333-1340.

Kuo, W., Lai, C., Huang, Y., Chang, C., & Kuo, Y. (2013). Balanced detection for spectral domain optical coherence tomography. *Optics Express, 21*(16), 19280-19280.

Larpthaveesarp, A., Ferriero, D., & Gonzalez, F. (2015). Growth Factors for the Treatment of Ischemic Brain Injury (Growth Factor Treatment). *Brain Sciences, 5*(2), 165-177.

Lee, S., Jeong, H., & Kim, B. (2010). High-speed spectral domain polarization- sensitive optical coherence tomography using a single camera and an optical switch at 1.3 μm. *Journal of Biomedical Optics, 15*(1), 010501-010501.

Leitgeba, R.A., Werkmeistera, R.M., Blattera, C., & Schmetterer L. (2014). Doppler Optical Coherence Tomography. *Progress in Retinal and Eye Research, 41*, 26-43.

Leong-Poi, H., Christiansen, J., Heppner, P., Lewis, C.W., Klibanov, A.L., Kaul, S., Lindner, J.R. (2005). Assessment of Endogenous and Therapeutic Arteriogenesis by Contrast Ultrasound Molecular Imaging of Integrin Expression. *Circulation, 111*(24), 3248-3254.

Libov, C., Optical coherence tomography more cost-effective than fluorescein angiogram in diagnosing macular disease. Medscape. Published: Apr 29, 2008. Retrieved: Jan 23, 2015.

Lucas, K.A., Pitari, G.M., Kazerounian, S., Ruiz-Stewart, I., Park, J., Schulz, S., Chepenik, K.P., & Waldman, S.A. (2000). Guanylyl cyclases and signaling by cyclic GMP. *Pharmacological Reviews, 52*(3), 375-414.

Luttun, A., & Carmeliet, P. (2014). Two faces of adult blood vessel formation: Vasculogenesis and angiogenesis. In Stem Cells: From Basic Research to Therapy, 2, 104-144. CRC Press.

Ma, Z. (2012). Practical approach for dispersion compensation in spectral-domain optical coherence tomography. *Optical Engineering, 51*(6), 063203-063203.

Macdonald, J. A., Murugesan, N., & Pachter, J. S. (2009). Endothelial cell heterogeneity of blood-brain barrier gene expression along the cerebral microvasculature. *Journal of Neuroscience Research, 88*(7), 1457-1474.

Maes, C., Carmeliet, G., & Schipani, E. (2012). Hypoxia-driven pathways in bone development, regeneration and disease. *Nature Reviews Rheumatology, 8*, 358-366.

Malinski, T., Bailey, F., Zhang, Z., & Chopp, M. (1993). Nitric oxide measured by a porphyrinic microsensor in rat brain after transient middle cerebral artery occlusion. *Journal of Cerebral Blood Flow & Metabolism, 13*(3), 355-358.

Markham, J.A., & Greenough, W.T. (2004). Experience-driven brain plasticity: beyond the synapse. *Neuron Glia Biology, 1*(4), 351-363.

Mayhan, W.G., Arrick, D.M., Sun, H., Patel, K.P. (2010). Exercise training restores impaired dilator responses of cerebral arterioles during chronic exposure to nicotine. *Journal of Applied Physiology, 109*(4), 1109-1114.

Michelson, A.A., & Morley, E.W. (1887). On the relative motion of the Earth and the luminiferous ether. *American Journal of Science, 34*, 333-345.

Michiels, C. (2004). Physiological and pathological responses to hypoxia. American Journal of Pathology, 164(6), 1875-1882.

Millauer, B., Wizigmann-Voos, S., Schnurch, H., Martinez, R., Moller, N.P., Risau, W., & Ullrich, A. (1993). High affinity VEGF binding and developmental expression suggest Flk-1 as a major regulator of vasculogenesis and angiogenesis. *Cell, 72*(6), 835-846.

Mouton, P. R. (2002). *Principles and practices of unbiased stereology: An introduction for bioscientists.* Baltimore: Johns Hopkins University Press.

Murohara, T., Horowitz, J., Silver, M., Tsurumi, Y., Chen, D., Sullivan, A., & Isner, J. (1998). Vascular endothelial growth factor/vascular permeability factor enhances vascular permeability via nitric oxide and prostacyclin. *Circulation, 97*(1), 99-107.

Neafsey, E.J. (1990). The complete ratunculus: output organization of layer v of the cerebral cortex. *Motor Systems*, 197-212.

Neafsey, E.J., Bold, E.L., Haas, G., Hurley-Gius, K.M., Quirk, G., Sievert, C.F., & Terreberry, R.R. (1986). The organization of the rat motor cortex: a microstimulation mapping study. *Brain Research, 396*(1), 77-96.

Nytko, K.J., Spielmann, P., Camenisch, G., Wenger, R.H., Stiehl, D.P. (2007). Regulated function of the prolyl-4-hydroxylase domain (PHD) oxygen sensor proteins. *Antioxidant and Redox Signaling, 9*(9), 1329-1338.

Ogunshola, O.O., Stewart, W.B., Mihalcik, V., Solli, T., Madri, J.A., & Ment, L.R. (2000). Neuronal VEGF expression correlates with angiogenesis in postnatal developing rat brain. *Developmental Brain Research, 119*(1), 139-153.

Papapetropoulos, A., García-Cardeña, G., Madri, J., & Sessa, W. (1997). Nitric oxide production contributes to the angiogenic properties of vascular endothelial growth factor in human endothelial cells. *Journal of Clinical Investigation, 100*(12), 3131-3139.

Pathway Central: ENOS Signaling. (2002-2012). Retrieved February 4, 2015, from: http://www.sabiosciences.com/pathway.php?sn=eNOS_Signaling

Patt, S., Sampaolo, S., Theallier-Janko, A., Tschairkin, I., & Cervos-Navarro, J. (1997). Cerebral angiogenesis triggered by severe chronic hypoxia displays regional differences. *Journal of Cerebral Blood Flow and Metabolism, 17*(7), 801-806.

Pekna, M., Pekny, M., Nilsson, M. (2012). Modulation of neural plasticity as a basis for stroke rehabilitation. *Stroke, 43*(10), 2819-28.

Pepper, M. (1997). Manipulating Angiogenesis: From Basic Science to the Bedside. *Arteriosclerosis, Thrombosis, and Vascular Biology, 17*, 605-619.

Perrey, S. (2013). Promoting motor function by exercising the brain. *Brain Science, 3*(1), 101-122.

Peters, K.G., De Vries, C., & Williams, L.T. (1993). Vascular endothelial growth factor receptor expression during embryogenesis and tissue repair suggests a role in endothelial differentiation and blood vessel growth. *Proceedings of the National Academy of Sciences of the United States of America, 90*(19), 8915-19.

Pryor, J.S., Montani, J.P., & Adair, T.H. (2010). Angiogenic gowth factor responses to long-term treadmill exercise in mice. *Indian Journal of Physiology and Pharmacology, 54*(4), 309-317.

Rasband, W.S. (1997-2016). ImageJ. *U.S. National Institutes of Health, Bethesda, Maryland, USA.* Retrieved from http://rsbweb.nih.gov/ij/index.html

Raoult, H., Bannier, E., Maurel, P., Neyton, C., Ferré, J.C., Schmitt, P., Barillot, C., & Gauvrit, J.Y. (2014). Hemodynamic quantification in brain arteriovenous malformations with time-resolved spin-labeled magneticresonance angiography. *Stroke, 45*(8), 2461-4.

Rhyu, I. J., Bytheway, J. A., Kohler, S. J., Lange, H., Lee, K. J., Boklewski, J., McCormick, K., Williams, N.I., Stanton, G.B., Greenough, W.T., & Cameron, J. L. (2010). Effects of aerobic exercise training on cognitive function and cortical vascularity in monkeys. *Neuroscience, 167*(4), 1239-1248.

Ribatti, D., & Crivellato, E. (2012). "Sprouting angiogenesis", a reappraisal. *Developmental Biology, 372*(2), 157-165.

Riddle, D.R., Sonntag, W.E., & Lichtenwainer, R.J. (2003). Microvascular plasticity in aging. *Aging Research Reviews, 2*(2), 149-168.

Rucker, H. K., Wynder, H. J., & Thomas, W. (2000). Cellular mechanisms of CNS pericytes. *Brain Research Bulletin, 51*(5), 363-369.

Rudic, R., Shesely, E., Maeda, N., Smithies, O., Segal, S., & Sessa, W. (1998). Direct evidence for the importance of endothelium-derived nitric oxide in vascular remodeling. *Journal of Clinical Investigation, 101*(4), 731-736.

Salceda, S., & Caro, J. (1997). Hypoxia-inducible factor 1alpha (HIF-1alpha) protein is rapidly degraded by ubiquitin-proteasome system under normoxic conditions. Its stabilization by hypoxia depends on redox-induced changes. The Journal of *Biological Chemistry, 272*(36), 22642-7.

Sanes, J., & Donoghue, J. (2000). Plasticity And Primary Motor Cortex. *Annual Review of Neuroscience, 23*, 393-415.

Schaper, W. (2009). Collateral circulation: Past and present. *Basic Research in Cardiology, 104*(1), 5-21.

Schierling, W., Troidl, K., Mueller, C., Troidl, C., Wustrack, H., Bachmann, G., Schmitz-Rixen, T. (2009). Increased intravascular flow rate triggers cerebral arteriogenesis. *Journal of Cerebral Blood Flow & Metabolism, 29*(4), 726-737.

Scholz, D., Ito, W., Fleming, I., Deindl, E., Sauer, A., Wiesnet, M., . . . Schaper, W. (2000). Ultrastructure and molecular histology of rabbit hind-limb collateral artery growth (arteriogenesis). *European Journal of Pathology, 436*(3), 257-270.

Shalaby, F., Rossant, J., Yamaguchi, T.P., Gertsenstein, M., Wu, X.F., Breitman, M.L., & Schuh, A.C. (1995). Failure of blood-island formation and vasculogenesis in Flk-1-deficient mice. *Nature, 376*(6535), 62-66.

Shamloo, A., Mohammadaliha, N., Heilshorn, S. C., & Bauer, A. L. (2015). A comparative study of collagen matrix density effect on endothelial sprout formation using experimental and computational approaches. *Annals of Biomedical Engineering, 44*(4), 929-941.

Shibuya, M. (2013). Vascular endothelial growth factor and its receptor system: physiological functions in angiogenesis and pathological roles in various diseases. *Journal of Biochemistry, 153*(1), 13-9.

Staton, C.A., Reed, M.W., & Brown, N.J. (2009). A critical analysis of current in vitro and in vivo angiogenesis assays. *International Journal of Experimental Pathology, 90*(3), 195-221.

Stratman, A.N., Davis, M.J., & Davis G.E. (2011). VEGF and FGF prime vascular tube morphogenesis and sprouting directed by hematopoietic stem cell cytokines. *Blood, 117*(14), 3709-3719.

Stroka, D.M., Burkhardt, T., Desbaillets, I., Wenger, R.H., Neil, D.A., Bauer, C., Gassmann, M., & Candinas, D. (2001). HIF-1 is expressed in normoxic tissue and displays an organ-specific regulation under systemic hypoxia. *FASEB Journal, 15*(13), 2445-2453.

Sugimura, T., Sako. K., Tohyama, Y., & Yonemasu, Y. (1998). Consecutive in vivo measurement of nitric oxide in transient forebrain ischemic rat under normothermia and hypothermia. *Brain Research, 808*, 313–316.

Swain, R.A., Harris, A.B., Wiener, E.C., Dutka, M.V., Morris, H.D., Theien, B.E., Konda, S., Engberg, K., Lauterbur, P.C., & Greenough, W.T. (2003). Prolonged exercise induces angiogenesis and increases cerebral blood volume in the primary motor cortex of the rat. *Neuroscience, 117*(4), 1037-1046.

Terry, S. Y., Abiraj, K., Frielink, C., Dijk, L. K., Bussink, J., Oyen, W. J., & Boerman, O. C. (2014). Imaging Integrin v 3 on Blood Vessels with 111In-RGD2 in Head and Neck Tumor Xenografts. *Journal of Nuclear Medicine, 55*(2), 281-286.

The top 10 causes of death. (2014). Accessed November 10, 2014.World Health Organization. Retrieved from: http://www.who.int/mediacentre/factsheets/fs310/en/

Thomas, A.G., Dennis, A., Bandettini, P.A., & Johansen-Berg, H. (2012). The effects of aerobic activity on brain structure. *Frontiers in Psychology, 3*, 86.

Thrippleton, M. (2015, September 25). Cerebrovascular-reactivity (CVR). Retrieved May 25, 2016, from http://www.ed.ac.uk/clinical-sciences/neuroimaging-sciences/about-us/imaging-techniques/cerebrovascular-reactivity

Ucuzian, A., Gassman, A., East, A., & Greisler, H. (2010). Molecular Mediators of Angiogenesis. *Journal of Burn Care & Research,* 158-175.

Van der Borght, K., Kóbor-Nyakas, D., Klauke, K., Eggen, B., Nyakas, C., Van der Zee, E., & Meerlo, P. (2009). Physical exercise leads to rapid adaptations in hippocampal vasculature: Temporal dynamics and relationship to cell proliferation and neurogenesis. *Hippocampus, 19*(10), 928-936.

Villringer, A., Them, A., Lindauer, U., Einhaupl, K., & Dirnagl, U. (1994). Capillary perfusion of the rat brain cortex: An in vivo confocal microscopy study. *Circulation Research, 75*(1), 55-62.

Voss, M.W., Vivar, C., Kramer, A.F., & van Praag. (2013). Bridging animal and human models of exercise-induced brain plasticity. *Trends in Cognitive Neuroscience, 17*(10), 525-44.

Wang, Z, & van Praag, H. (2012). Exercise and the brain: Neurogenesis, synaptic plasticity, spine density, and angiogenesis. Functional Imaging in Exercise and Sports Sciences, p3-24. New York, NY: Springer.

Wang-Fischer, Y., & Koetzner, L. (2009). Brain Hemorrhage Models in Rodents. In Y. Wang-Fischer (Ed.), Manual of Stroke Models in Rats. Boca Raton: CRC Press.

Willems, P.W., Taeshineetanakul, P., Schnek, B., Brouwer, P.A., Terbrugge, K.G., & Krings, T. (2012). The use of 4D-CTA in the diagnostic work-up of brain arteriovenous malformations. *Neuroradiology, 54*(2),123-131.

Winter, B., Breitenstein, C., Mooren, F. C., Voelker, K., Fobker, M., Lechterman, A., Krueger, K., Fromme, A., Korsukewitz, C., Floel, A., & Knecht, S. (2007). High impact running improves learning. *Neurobiology of Learning and Memory, 87*, 597-609.

Yaqoob, Z., Wu, J., & Yang, C. (2005). Spectral domain optical coherence tomography: A better OCT imaging strategy. *Biotechniques, 39*(6), 6-13.

Yazdan-Shahmorad, A., Lehmkuhle, M., Gage, G., Marzullo, T., Parikh, H., Miriani, R., & Kipke, D. (2011). Estimation of electrode location in a rat motor cortex by laminar analysis of electrophysiology and intracortical electrical stimulation. *Journal of Neural Engineering, 8*, 046018-046018.

Yezhuvath, U. S., Lewis-Amezcua, K., Varghese, R., Xiao, G., & Lu, H. (2009). On the assessment of cerebrovascular reactivity using hypercapnia BOLD MRI. *NMR in Biomedicine, 22*(7), 779-786.

Young, N.A., Collins, C.E., & Kaas, J.H. (2013). Cell and neuron densities in the primary motor cortex of primates. *Frontiers in Neural Circuits, 7*, 30.

Zajko, W., Kramer, A., & Poon, L. (2009). Enhancing cognitive functioning and brain plasticity (Vol. 3). Champaign, IL: Human Kinetics.

Zeiher, A.M., Krause, T., Schachinger, V., Minners, J., & Moser, E. (1995). Impaired endothelium-dependent vasodilation of coronary resistance vessels is associated with exercise-induced myocardial ischemia. *Circulation, 91*(9), 2345-52.

Zhang, P., Yu, H., Zhou, N., Zhang, J., Wu, Y., Zhang, Y., . . . Hu, Y. (2013). Early exercise improves cerebral blood flow through increased angiogenesis in experimental stroke rat model. *Journal of Neuroengineering and Rehabilitation, 10*(1), 43.

Zheng, X., Ruas, J.L., Cao, R., Salomons F.A., Cao, Y., Poellinger, L., & Pereira, T. (2006). Cell-type-specific regulation of degradation of hypoxia-inducible factor 1 alpha: role of subcellular compartmentalization. *Molecular and Cellular Biology, 26*(12), 4628-41.

Zhu, J., Dugas-Ford, J., Chang, M., Purta, P., Han, K., Hong, Y., . . . Azar, D. T. (2015). Simultaneous in vivo imaging of blood and lymphatic vessel growth in Prox1-GFP/Flk1::myr-mCherry mice. *FEBS Journal, 282*(8), 1458-1467.

Zohdi, T.I., & Kuypers, F.A. (2006). Modeling and rapid simulation of multiple red blood cell light scattering. *Journal of the Royal Society, 3*(11), 823-31.